REPORT ON A HELICOPTER-BORNE VERSATILE TIME DOMAIN ELECTROMAGNETIC (VTEM^{plus}) AND HORIZONTAL MAGNETIC GRADIOMETER GEOPHYSICAL SURVEY

Otter Block

Timmins, Ontario

For:

Fletcher Nickel Inc.

By:

Geotech Ltd.

245 Industrial Parkway North

Aurora, Ont., CANADA, L4G 4C4

Tel: 1.905.841.5004

Fax: 1.905.841.0611

www.geotech.ca

Email: info@geotech.ca

Survey flown during September 2012

Project 12099

September, 2012

TABLE OF CONTENTS

LIST OF FIGURES

LIST OF TABLES

APPENDICES

REPORT ON A HELICOPTER-BORNE VERSATILE TIME DOMAIN ELECTROMAGNETIC (VTEM^{plus}) and HORIZONTAL MAGNETIC GRADIOMETER GEOPHYSICAL SURVEY

Otter Block
Timmins, Ontario

EXECUTIVE SUMMARY

During Septebmer 14th to September 19th 2012 Geotech Ltd. carried out a helicopter-borne geophysical survey over the Otter Block situated approximately 53 km southeast of Timmins, Ontario, Canada.

Principal geophysical sensors included a versatile time domain electromagnetic (VTEM^{plus}) system, and horizontal magnetic gradiometer. Ancillary equipment included a GPS navigation system and a radar altimeter. A total of 378.2 line-kilometres of geophysical data were acquired during the survey.

In-field data quality assurance and preliminary processing were carried out on a daily basis during the acquisition phase. Preliminary and final data processing, including generation of final digital data and map products were undertaken from the office of Geotech Ltd. in Aurora, Ontario.

The processed survey results are presented as the following maps:

- Electromagnetic stacked profiles of dB/dt Z Components,
- B-Field Z Component Channel grid
- Total Magnetic Intensity (TMI),

Digital data includes all electromagnetic and magnetic products, plus ancillary data including the waveform.

The survey report describes the procedures for data acquisition, processing, final image presentation and the specifications for the digital data set.

1. INTRODUCTION

1.1 General Considerations

Geotech Ltd. performed a helicopter-borne geophysical survey over the Otter Block located approximately 53 km southeast of Timmins, Ontario (Figure 1 & 2).

Joerg Kleinboeck represented Fletcher Nickel Inc. during the data acquisition and data processing phases of this project.

The geophysical surveys consisted of helicopter borne EM using the versatile time-domain electromagnetic (VTEM^{plus}) system with Z and X component measurements and horizontal magnetic gradiometer using two cesium magnetometers. A total of 378.2 line-km of geophysical data were acquired during the survey.

The crew was based out of Timmins (Figure 2) in Ontario for the acquisition phase of the survey. Survey flying started on September 14th and was completed on September 19th, 2012

Data quality control and quality assurance, and preliminary data processing were carried out on a daily basis during the acquisition phase of the project. Final data processing followed immediately after the end of the survey. Final reporting, data presentation and archiving were completed from the Aurora office of Geotech Ltd. in September, 2012.

Figure 1: Property Location.

1.2 Survey and System Specifications

The survey area is located approximately 53 kilometres southeast of Timmins, Ontario (Figure 2).

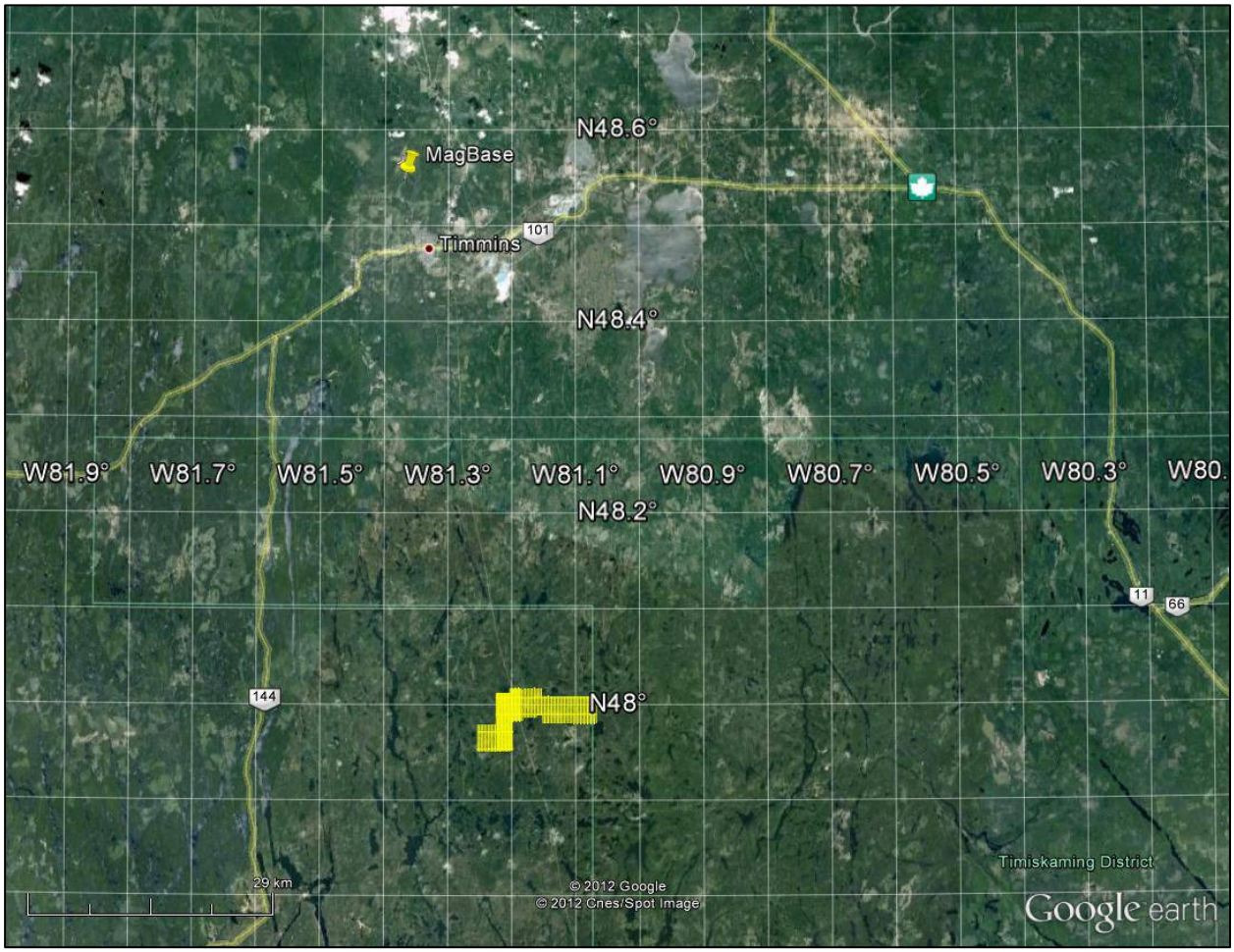

Figure 2: Survey area location on Google Earth.

The block was flown in a north to south (N 0° E azimuth) direction with traverse line spacing of 100/200 metres as depicted in Figure 3. Tie lines were flown perpendicular to the traverse lines at a spacing of 2000 metres respectively. For more detailed information on the flight spacing and direction see Table 1.

1.3 Topographic Relief and Cultural Features

Topographically, the block exhibits a shallow relief with an elevation ranging from 345 to 390 metres above mean sea level over an area of 51 square kilometres (Figure 3).

There are various rivers and streams running through the survey area which connect various lakes and wetlands. There are visible signs of culture such as roads, railways and powerlines which run throughout the centre of the survey area.

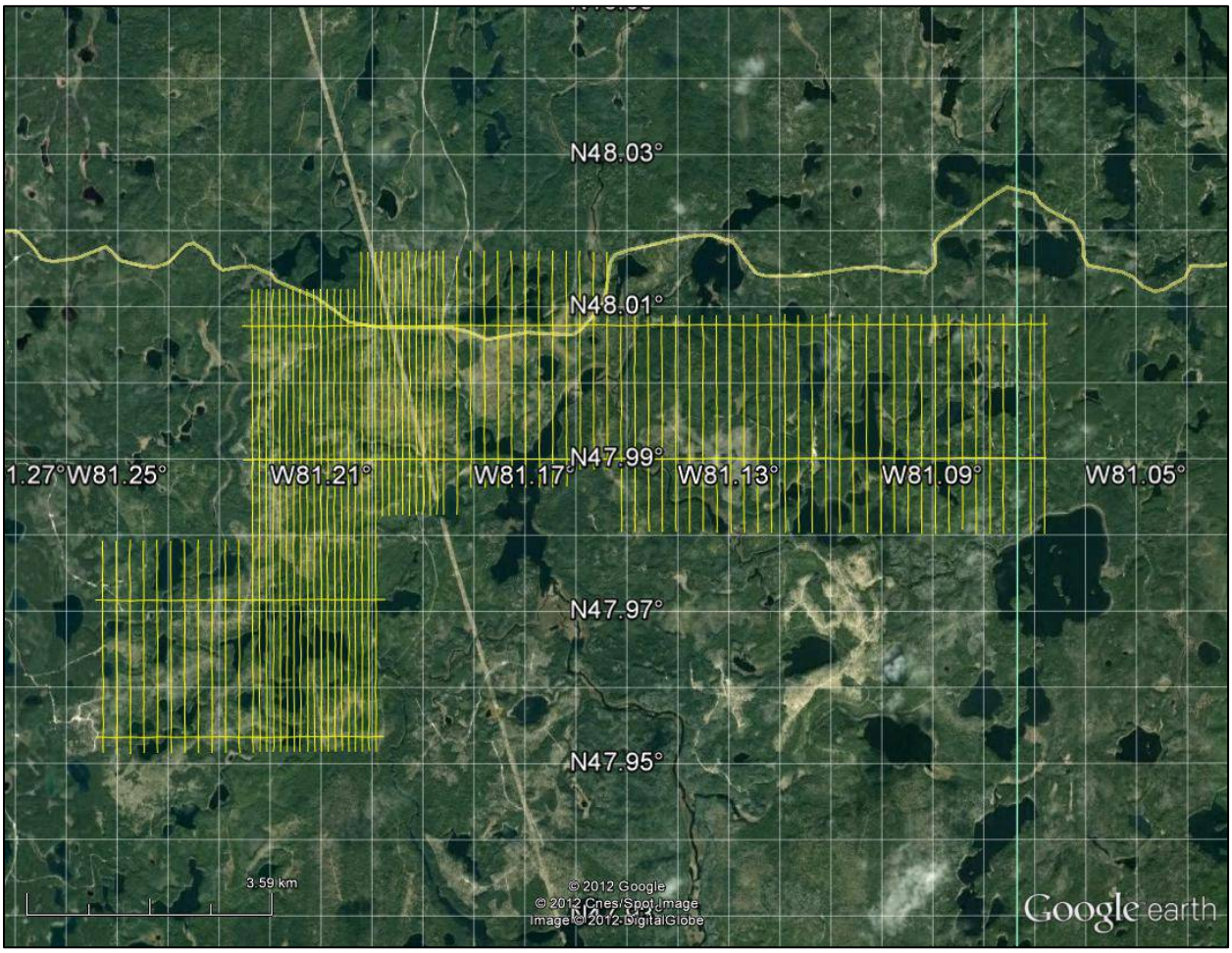

Figure 3: Flight path over a Google Earth Image.

The survey area is covered by numerous mining claims, which are shown in Appendix A, and are plotted on all maps. The survey area is covered by NTS (National Topographic Survey) of Canada sheets 041P14 & 042A03.

2. DATA ACQUISITION

2.1 Survey Area

The survey block (see Figure 3 and Appendix A) and general flight specifications are as follows:

Table 1: Survey Specifications

Survey block	Traverse Line spacing (m)	Area (Km^2)	Planned[1] Line-km	Actual Line-km	Flight direction	Line numbers
Otter Block	Traverse: 100/200	51	365.4	346	N 0° E / N 180° E	L1000-L1690
	Tie: 1000			32.2	N90° E / N 270° E	T1800-T1830
TOTAL		**51**	**365.4**	**378.2**		

Survey block boundaries co-ordinates are provided in Appendix B.

2.2 Survey Operations

Survey operations were based out of Timmins in Ontario from September 14th to September 19th, 2012. The following table shows the timing of the flying.

Table 2: Survey schedule

Date	Flight #	Flow km	Block	Crew location	Comments
14-Sep-2012				Timmins,ON	mobilization
15-Sep-2012				Timmins,ON	Crew arrived on site and system assembly
16-Sep-2012	1,2	281		Timmins,ON	281km flown
17-Sep-2012				Timmins,ON	No production due to weather
18-Sep-2012				Timmins,ON	No production due to weather
19-Sep-2012	3	85		Timmins,ON	Remaining kms were flown – flying complete

[1] Note: Actual Line kilometres represent the total line kilometres in the final database. These line-km normally exceed the planned line-km, as indicated in the survey NAV files.

2.3 Flight Specifications

During the survey the helicopter was maintained at a mean altitude of 74 metres above the ground with an average survey speed of 80 km/hour. This allowed for an actual average EM bird terrain clearance of 41 metres and a magnetic sensor clearance of 50 metres.

The on board operator was responsible for monitoring the system integrity. He also maintained a detailed flight log during the survey, tracking the times of the flight as well as any unusual geophysical or topographic features.

On return of the aircrew to the base camp the survey data was transferred from a compact flash card (PCMCIA) to the data processing computer. The data were then uploaded via ftp to the Geotech office in Aurora for daily quality assurance and quality control by qualified personnel.

2.4 Aircraft and Equipment

2.4.1 Survey Aircraft

The survey was flown using a Eurocopter Aerospatiale (Astar) 350 B3 helicopter, registration C-FVTM. The helicopter is owned and operated by Geotech Aviation. Installation of the geophysical and ancillary equipment was carried out by a Geotech Ltd crew.

2.4.2 Electromagnetic System

The electromagnetic system was a Geotech Time Domain EM (VTEM^{plus}) system. VTEM with the Serial number 8 had been used for the survey. The configuration is as indicated in Figure 5.

The VTEM Receiver and transmitter coils were in concentric-coplanar and Z-direction oriented configuration. The receiver system for the project also included a coincident-coaxial X-direction coil to measure the in-line dB/dt and calculate B-Field responses. The EM bird was towed at a mean distance of 35 metres below the aircraft as shown in Figure 5. The receiver decay recording scheme is shown diagrammatically in Figure 4.

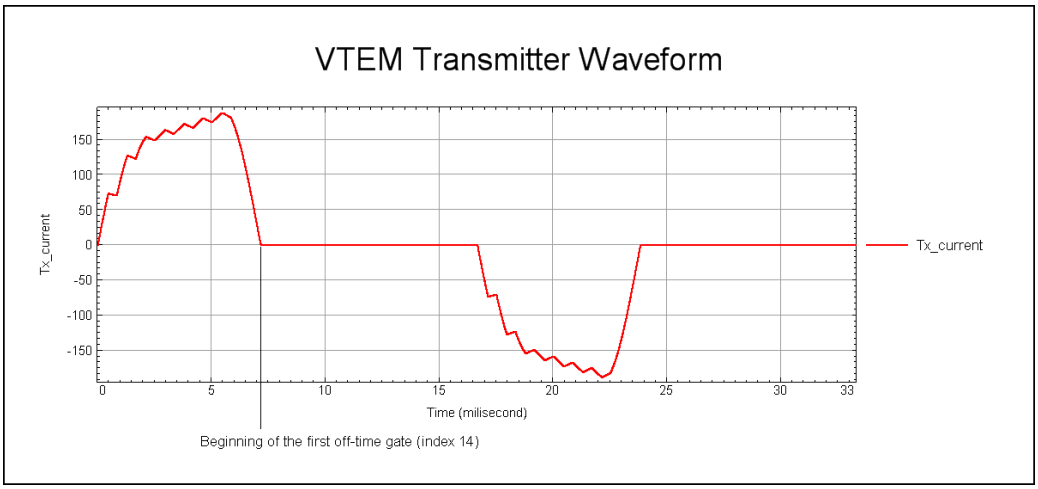

Figure 4: VTEM Waveform & Sample Times.

The VTEM decay sampling scheme is shown in Table 3 below. Thirty-two time measurement gates were used for the final data processing in the range from 0.096 to 7.036 msec.

Table 3: Off-Time Decay Sampling Scheme

VTEM Decay Sampling Scheme			
Index	**Middle**	**Start**	**End**
Milliseconds			
14	0.096	0.090	0.103
15	0.110	0.103	0.118
16	0.126	0.118	0.136
17	0.145	0.136	0.156
18	0.167	0.156	0.179
19	0.192	0.179	0.206
20	0.220	0.206	0.236
21	0.253	0.236	0.271
22	0.290	0.271	0.312
23	0.333	0.312	0.358
24	0.383	0.358	0.411
25	0.440	0.411	0.472
26	0.505	0.472	0.543
27	0.580	0.543	0.623
28	0.667	0.623	0.716
29	0.766	0.716	0.823
30	0.880	0.823	0.945
31	1.010	0.945	1.086
32	1.161	1.086	1.247
33	1.333	1.247	1.432
34	1.531	1.432	1.646
35	1.760	1.646	1.891
36	2.021	1.891	2.172
37	2.323	2.172	2.495
38	2.667	2.495	2.865
39	3.063	2.865	3.292
40	3.521	3.292	3.781
41	4.042	3.781	4.341
42	4.641	4.341	4.987
43	5.333	4.987	5.729
44	6.125	5.729	6.581
45	7.036	6.581	7.560

Z Component: 14-45 time gates
X Component: 20-45 time gates.

VTEM system specifications:

Transmitter

- Transmitter coil diameter: 26 m
- Number of turns: 4
- Effective Transmitter coil area: 2123 m^2
- Transmitter base frequency: 30 Hz
- Peak current: 188 A
- Pulse width: 5.879 ms
- Wave form shape: Bi-polar trapezoid
- Peak dipole moment: 399,258 nIA
- Actual average EM Bird terrain clearance: 41 metres above the ground

Receiver

- X Coil diameter: 0.32 m
- Number of turns: 245
- Effective coil area: 19.69 m^2
- Z-Coil coil diameter: 1.2 m
- Number of turns: 100
- Effective coil area: 113.04 m^2

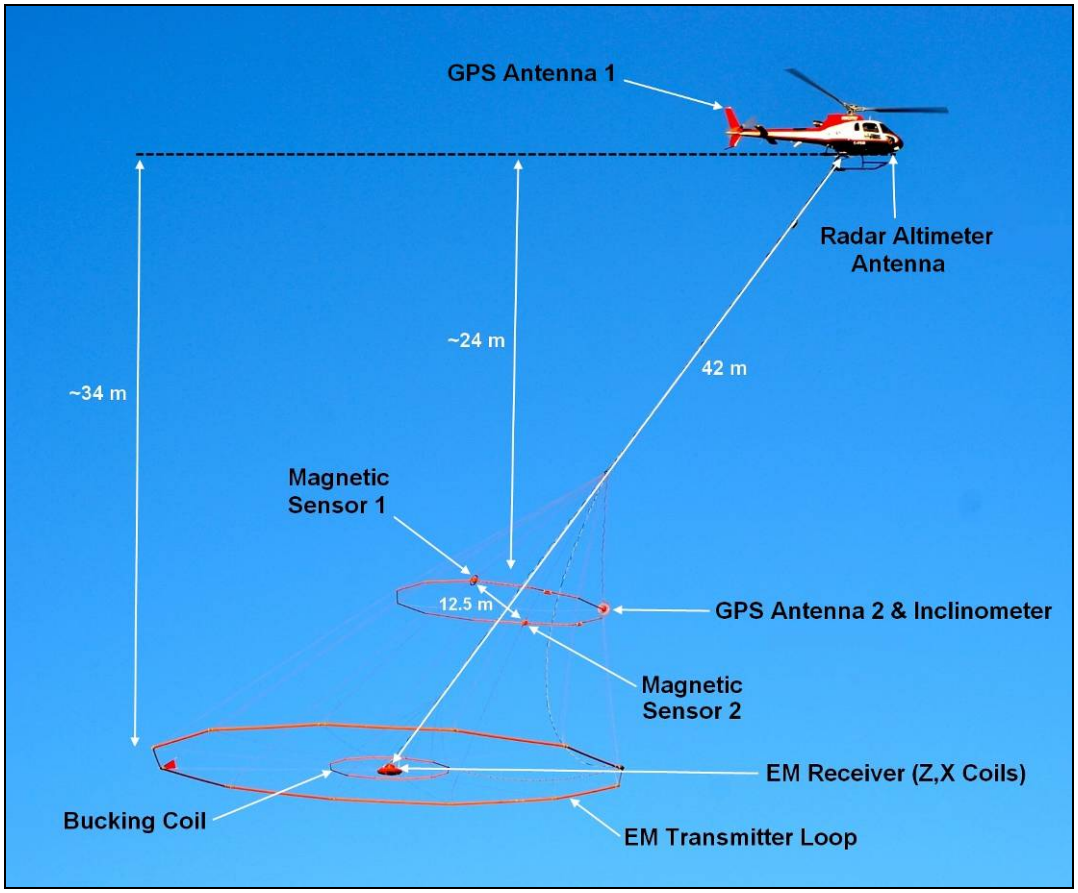

Figure 5: VTEM^{plus} System Configuration.

2.4.3 Horizontal Magnetic Gradiometer

The horizontal magnetic gradiometer consists of two Geometrics split-beam field magnetic sensors with a sampling interval of 0.1 seconds. These sensors are mounted 12.5 metres apart on a separate loop, 10 metres above the EM bird. A GPS antenna and Gyro Inclinometer is installed on the separate loop to accurately record the tilt and position of the magnetic gradiomag bird.

2.4.4 Radar Altimeter

A Terra TRA 3000/TRI 40 radar altimeter was used to record terrain clearance. The antenna was mounted beneath the bubble of the helicopter cockpit (Figure 5).

2.4.5 GPS Navigation System

The navigation system used was a Geotech PC104 based navigation system utilizing a NovAtel's WAAS (Wide Area Augmentation System) enabled GPS receiver, Geotech navigate software, a full screen display with controls in front of the pilot to direct the flight and a NovAtel GPS antenna mounted on the helicopter tail (Figure 5). As many as 11 GPS and two WAAS satellites may be monitored at any one time. The positional accuracy or circular error probability (CEP) is 1.8 m, with WAAS active, it is 1.0 m. The co-ordinates of the block were set-up prior to the survey and the information was fed into the airborne navigation system. The second GPS antenna is installed on the additional magnetic loop together with Gyro Inclinometer.

2.4.6 Digital Acquisition System

A Geotech data acquisition system recorded the digital survey data on an internal compact flash card. Data is displayed on an LCD screen as traces to allow the operator to monitor the integrity of the system. The data type and sampling interval as provided in Table 4.

Table 4: Acquisition Sampling Rates

Data Type	Sampling
TDEM	0.1 sec
Magnetometer	0.1 sec
GPS Position	0.2 sec
Radar Altimeter	0.2 sec
Inclinometer	0.1 sec

2.5 Base Station

A combined magnetometer/GPS base station was utilized on this project. A Geometrics Cesium vapour magnetometer was used as a magnetic sensor with a sensitivity of 0.001 nT. The base station was recording the magnetic field together with the GPS time at 1 Hz on a base station computer.

The base station magnetometer sensor was installed at the end of a dirt road (48º32'8612"N, 81º22'2415"W); away from electric transmission lines and moving ferrous objects such as motor vehicles. The base station data were backed-up to the data processing computer at the end of each survey day.

3. PERSONNEL

The following Geotech Ltd. personnel were involved in the project.

Field:

Project Manager:	Adrian Sarmasag (Office)
Data QC:	Neil Fiset (Office)
Crew chief:	John West-Fiset
Operator:	Rick Gotuzzo

The survey pilot and the mechanical engineer were employed directly by the helicopter operator – Geotech Aviation

Pilot:	Geoffrey Rawlins
Mechanical Engineer:	n/a

Office:

Preliminary Data Processing:	Neil Fiset
Final Data Processing:	Marta Orta
Final Data QA/QC:	Alexander Prikhodko
Reporting/Mapping:	Corrie Laver

Data acquisition phase was carried out under the supervision of Andrei Bagrianski, P. Geo, Chief Operating Officer. Processing and Interpretation phases were carried out under the supervision of Alexander Prikhodko, P. Geo, Senior Geophysicist, VTEM Interpretation Supervisor. The customer relations were looked after by Paolo Berardelli.

4. DATA PROCESSING AND PRESENTATION

Data compilation and processing were carried out by the application of Geosoft OASIS Montaj and programs proprietary to Geotech Ltd.

4.1 Flight Path

The flight path, recorded by the acquisition program as WGS 84 latitude/longitude, was converted into the NAD83 Datum, UTM Zone 17 North coordinate system in Oasis Montaj.

The flight path was drawn using linear interpolation between x, y positions from the navigation system. Positions are updated every second and expressed as UTM easting's (x) and UTM northing's (y).

4.2 Electromagnetic Data

A three stage digital filtering process was used to reject major sferic events and to reduce noise levels. Local sferic activity can produce sharp, large amplitude events that cannot be removed by conventional filtering procedures. Smoothing or stacking will reduce their amplitude but leave a broader residual response that can be confused with geological phenomena. To avoid this possibility, a computer algorithm searches out and rejects the major sferic events.

The signal to noise ratio was further improved by the application of a low pass linear digital filter. This filter has zero phase shift which prevents any lag or peak displacement from occurring, and it suppresses only variations with a wavelength less than about 1 second or 15 metres. This filter is a symmetrical 1 sec linear filter.

The results are presented as stacked profiles of EM voltages for the time gates, in linear - logarithmic scale for the B-field Z component and dB/dt responses in the Z and X components. B-field Z component time channel recorded at 6.125 milliseconds after the termination of the impulse is also presented as a colour image. Fraser Filter X component is also presented as a colour image. Calculated Time Constant (TAU) with anomaly contours of Calculated Vertical Derivative of TMI is presented in Appendix C and E. Resistivity Depth Image (RDI) is also presented in Appendix E and F.

VTEM has two receiver coil orientations. Z-axis coil is oriented parallel to the transmitter coil axis and both are horizontal to the ground. The X-axis coil is oriented parallel to the ground and along the line-of-flight. This combined two coil configuration provides information on the position, depth, dip and thickness of a conductor. Generalized modeling results of VTEM data, are shown in Appendix D.

In general X-component data produce cross-over type anomalies: from "+ to – "in flight direction of flight for "thin" sub vertical targets and from "- to +" in direction of flight for "thick" targets. Z component data produce double peak type anomalies for "thin" sub vertical targets and single peak for "thick" targets.

The limits and change-over of "thin-thick" depends on dimensions of a TEM system (Appendix D, Figure D-16).

Because of X component polarity is under line-of-flight, convolution Fraser Filter (Figure 6) is applied to X component data to represent axes of conductors in the form of grid map. In this case positive FF anomalies always correspond to “plus-to-minus” X data crossovers independent of the flight direction.

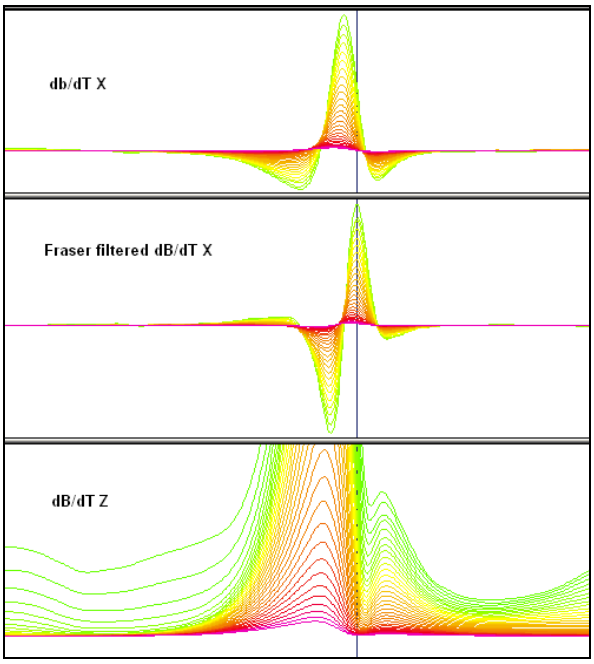

Figure 6: Z, X and Fraser filtered X (FFx) components for “thin” target.

4.3 Horizontal Magnetic Gradiometer Data

The horizontal gradients data from the VTEM^{plus} are measured by two magnetometers 12.5 m apart on an independent bird mounted10m above the VTEM loop. A GPS and a Gyro Inclinometer help to determine the positions and orientations of the magnetometers. The data from the two magnetometers are corrected for position and orientation variations, as well as for the diurnal variations using the base station data.

The position of the centre of the horizontal magnetic gradiometer bird is calculated form the GPS utilizing in-house processing tool in Geosoft. Following that total magnetic intensity is calculated at the center of the bird by calculating the mean values from both sensors. In addition to the total intensity advanced processing is done to calculate the in-line and cross-line (or lateral) horizontal gradient which enhance the understanding of magnetic targets. The in-line (longitudinal) horizontal gradient is calculated from the difference of two consecutive total magnetic field readings divided by the distance along the flight line direction, while the cross-line (lateral) horizontal magnetic gradient is calculated from the difference in the magnetic readings from both magnetic sensors divided by their horizontal separation.

Two advanced magnetic derivative products, the total horizontal derivative (THDR), and tilt angle derivative and are also created. The total horizontal derivative or gradient is also called the analytic signal, is defined as:

THDR = sqrt(Hx*Hx+Hy*Hy), where Hx and Hy are cross-line and in-line horizontal gradients.

The tilt angle derivative (TDR) is defined as:

TDR = arctan(Vz/THDR), where THDR is the total horizontal derivative, and Vz is the vertical derivative.

Measured cross-line gradients can help to enhance cross-line linear features during gridding.

5. DELIVERABLES

5.1 Survey Report

The survey report describes the data acquisition, processing, and final presentation of the survey results. The survey report is provided in two paper copies and digitally in PDF format.

5.2 Maps

Final maps were produced at scale of 1:20,000 for best representation of the survey size and line spacing. The coordinate/projection system used was NAD83 Datum, UTM Zone 17 North. All maps show the mining claims, flight path trace and topographic data; latitude and longitude are also noted on maps.

The preliminary and final results of the survey are presented as EM profiles, a late-time gate gridded EM channel, and a colour magnetic TMI contour map. The following maps are presented on paper;

- VTEM dB/dt profiles Z Component, Time Gates 0.220 – 7.036 ms in linear – logarithmic scale.
- VTEM B-field late time Z Component colour image.
- Total magnetic intensity (TMI) colour image and contours.

5.3 Digital Data

Two copies of the data and maps on DVD were prepared to accompany the report. Each DVD contains a digital file of the line data in GDB Geosoft Montaj format as well as the maps in Geosoft Montaj Map and PDF format.

- DVD structure.

  Data contains databases, grids and maps, as described below.
  Report contains a copy of the report and appendices in PDF format.

  Databases in Geosoft GDB format, containing the channels listed in Table 5.

Table 5: Geosoft GDB Data Format

Channel name	Units	Description
X:	metres	UTM Easting NAD83 Zone 17 North
Y:	metres	UTM Northing NAD83 Zone 17 North
Longitude:	Decimal Degrees	WGS 84 Longitude data
Latitude:	Decimal Degrees	WGS 84 Latitude data
Z:	metres	GPS antenna elevation (above Geoid)
Radar:	metres	helicopter terrain clearance from radar altimeter
Radarb:	metres	Calculated EM bird terrain clearance from radar altimeter
DEM:	metres	Digital Elevation Model
Gtime:	Seconds of the day	GPS time
Mag1L:	nT	Measured Total Magnetic field data (left sensor)
Mag1R:	nT	Measured Total Magnetic field data (right sensor)
Basemag:	nT	Magnetic diurnal variation data
Mag2LZ	nT	Z corrected (w.r.t. loop center) and diurnal corrected magnetic field left mag
Mag2RZ	nT	Z corrected (w.r.t. loop center) and diurnal corrected magnetic field right mag
TMI2	nT	Calculated from diurnal corrected total magnetic field intensity of the centre of the loop
TMI3	nT	Microleveled total magnetic field intensity of the centre of the loop
Hgcxline		measured cross-line gradient
Hginline		Calculated in-line gradient
CVG	nT/m	Calculated Magnetic Vertical Gradient
SFz[14]:	$pV/(A*m^4)$	Z dB/dt 0.096 millisecond time channel
SFz[15]:	$pV/(A*m^4)$	Z dB/dt 0.110 millisecond time channel
SFz[16]:	$pV/(A*m^4)$	Z dB/dt 0.126 millisecond time channel
SFz[17]:	$pV/(A*m^4)$	Z dB/dt 0.145 millisecond time channel
SFz[18]:	$pV/(A*m^4)$	Z dB/dt 0.167 millisecond time channel
SFz[19]:	$pV/(A*m^4)$	Z dB/dt 0.192 millisecond time channel
SFz[20]:	$pV/(A*m^4)$	Z dB/dt 0.220 millisecond time channel
SFz[21]:	$pV/(A*m^4)$	Z dB/dt 0.253 millisecond time channel
SFz[22]:	$pV/(A*m^4)$	Z dB/dt 0.290 millisecond time channel
SFz[23]:	$pV/(A*m^4)$	Z dB/dt 0.333 millisecond time channel
SFz[24]:	$pV/(A*m^4)$	Z dB/dt 0.383 millisecond time channel
SFz[25]:	$pV/(A*m^4)$	Z dB/dt 0.440 millisecond time channel
SFz[26]:	$pV/(A*m^4)$	Z dB/dt 0.505 millisecond time channel
SFz[27]:	$pV/(A*m^4)$	Z dB/dt 0.580 millisecond time channel
SFz[28]:	$pV/(A*m^4)$	Z dB/dt 0.667 millisecond time channel
SFz[29]:	$pV/(A*m^4)$	Z dB/dt 0.766 millisecond time channel
SFz[30]:	$pV/(A*m^4)$	Z dB/dt 0.880 millisecond time channel
SFz[31]:	$pV/(A*m^4)$	Z dB/dt 1.010 millisecond time channel
SFz[32]:	$pV/(A*m^4)$	Z dB/dt 1.161 millisecond time channel
SFz[33]:	$pV/(A*m^4)$	Z dB/dt 1.333 millisecond time channel
SFz[34]:	$pV/(A*m^4)$	Z dB/dt 1.531 millisecond time channel
SFz[35]:	$pV/(A*m^4)$	Z dB/dt 1.760 millisecond time channel
SFz[36]:	$pV/(A*m^4)$	Z dB/dt 2.021 millisecond time channel
SFz[37]:	$pV/(A*m^4)$	Z dB/dt 2.323 millisecond time channel
SFz[38]:	$pV/(A*m^4)$	Z dB/dt 2.667 millisecond time channel
SFz[39]:	$pV/(A*m^4)$	Z dB/dt 3.063 millisecond time channel
SFz[40]:	$pV/(A*m^4)$	Z dB/dt 3.521 millisecond time channel
SFz[41]:	$pV/(A*m^4)$	Z dB/dt 4.042 millisecond time channel

Channel name	Units	Description
SFz[42]:	pV/(A*m^4)	Z dB/dt 4.641 millisecond time channel
SFz[43]:	pV/(A*m^4)	Z dB/dt 5.333 millisecond time channel
SFz[44]:	pV/(A*m^4)	Z dB/dt 6.125 millisecond time channel
SFz[45]:	pV/(A*m^4)	Z dB/dt 7.036 millisecond time channel
SFx[20]:	pV/(A*m^4)	X dB/dt 0.220 millisecond time channel
SFx[21]:	pV/(A*m^4)	X dB/dt 0.253 millisecond time channel
SFx[22]:	pV/(A*m^4)	X dB/dt 0.290 millisecond time channel
SFx[23]:	pV/(A*m^4)	X dB/dt 0.333 millisecond time channel
SFx[24]:	pV/(A*m^4)	X dB/dt 0.383 millisecond time channel
SFx[25]:	pV/(A*m^4)	X dB/dt 0.440 millisecond time channel
SFx[26]:	pV/(A*m^4)	X dB/dt 0.505 millisecond time channel
SFx[27]:	pV/(A*m^4)	X dB/dt 0.580 millisecond time channel
SFx[28]:	pV/(A*m^4)	X dB/dt 0.667 millisecond time channel
SFx[29]:	pV/(A*m^4)	X dB/dt 0.766 millisecond time channel
SFx[30]:	pV/(A*m^4)	X dB/dt 0.880 millisecond time channel
SFx[31]:	pV/(A*m^4)	X dB/dt 1.010 millisecond time channel
SFx[32]:	pV/(A*m^4)	X dB/dt 1.161 millisecond time channel
SFx[33]:	pV/(A*m^4)	X dB/dt 1.333 millisecond time channel
SFx[34]:	pV/(A*m^4)	X dB/dt 1.531 millisecond time channel
SFx[35]:	pV/(A*m^4)	X dB/dt 1.760 millisecond time channel
SFx[36]:	pV/(A*m^4)	X dB/dt 2.021 millisecond time channel
SFx[37]:	pV/(A*m^4)	X dB/dt 2.323 millisecond time channel
SFx[38]:	pV/(A*m^4)	X dB/dt 2.667 millisecond time channel
SFx[39]:	pV/(A*m^4)	X dB/dt 3.063 millisecond time channel
SFx[40]:	pV/(A*m^4)	X dB/dt 3.521 millisecond time channel
SFx[41]:	pV/(A*m^4)	X dB/dt 4.042 millisecond time channel
SFx[42]:	pV/(A*m^4)	X dB/dt 4.641 millisecond time channel
SFx[43]:	pV/(A*m^4)	X dB/dt 5.333 millisecond time channel
SFx[44]:	pV/(A*m^4)	X dB/dt 6.125 millisecond time channel
SFx[45]:	pV/(A*m^4)	X dB/dt 7.036 millisecond time channel
BFz	(pV*ms)/(A*m^4)	Z B-Field data for time channels 14 to 45
BFx	(pV*ms)/(A*m^4)	X B-Field data for time channels 20 to 45
SFxFF	pV/(A*m^4)	Fraser Filtered X dB/dt
Nchan_BF		Latest time channels of TAU calculation
Nchan_SF		Latest time channels of TAU calculation
Tau_BF	ms	Time constant B-Field
Tau_SF	ms	Time constant dB/dt
PLM:		60 Hz power line monitor

Electromagnetic B-field and dB/dt Z component data is found in array channel format between indexes 14 – 45, and X component data from 20 – 45, as described above.

- Database of the Resistivity Depth Images in Geosoft GDB format, containing the following channels:

- Database of the VTEM Waveform “12099_waveform_final.gdb” in Geosoft GDB format, containing the following channels:

  Time: Sampling rate interval, 5.2083 milliseconds
  Rx_Volt: Output voltage of the receiver coil (Volt)
  Tx_Current: Output current of the transmitter (Amp)

A Geosoft .GRD file has a .GI metadata file associated with it, containing grid projection information. A grid cell size of 25 metres was used.

- Maps at 1:20,000 in Geosoft MAP format, as follows:

12099_20k_dBdt:	dB/dt profiles Z Component, Time Gates 0.220 – 7.036 ms in linear – logarithmic scale.
12099_20k_BFz44:	B-field late time Z Component Channel 44, Time Gate 6.125 ms colour image.
12099_20k_TMI:	Total magnetic intensity (TMI) colour image and contours.

Maps are also presented in PDF format.

- 1:50,000 topographic vectors were taken from the NRCAN Geogratis database at; http://geogratis.gc.ca/geogratis/en/index.html.

6. CONCLUSIONS AND RECOMMENDATIONS

A helicopter-borne versatile time domain electromagnetic (VTEM) geophysical survey has been completed over the Otter Block near Timmins, Ontario.

The total area coverage is 51 km^2. Total survey line coverage is 378.2 line kilometres. The principal sensors included a Time Domain EM system and horizontal magnetic gradiometer using two cesium magnetometers. Results have been presented as stacked profiles, and contour colour images at a scale of 1:20,000. A formal Interpretation has not been included or requested.

Based on the geophysical results obtained, a number of TEM anomalies are identified across the property. Identified electromagnetic anomalies are visible in all time gates range, in dBz/dt and B-field data, with consistent response in the X and Z coil data.

Power lines are identified across the property. Caution is recommended during further interpretation; as such cultural components might affect the geological response inherent in the data

It is recommended picking anomalies with conductance grading and center localization of the targets, detail resistivity depth imaging, and plate Maxwell modelling prior to ground follow up and drill testing. If magnetic anomalies are of interest, 3D inversion and/or modeling of magnetic field is recommended as well.

Respectfully submitted[2],

Neil Fiset
Geotech Ltd.

Marta Orta
Geotech Ltd.

Alexander Prikhodko, P. Geo
Geotech Ltd.

September, 2012

[2] Final data processing of the EM and magnetic data were carried out by Neil Fiset and Marta Orta from the office of Geotech Ltd. in Aurora, Ontario, under the supervision of Alexander Prikhodko, P.Geo., PhD, Senior Geophysicist, VTEM Interpretation Supervisor.

APPENDIX A

SURVEY BLOCK LOCATION MAP

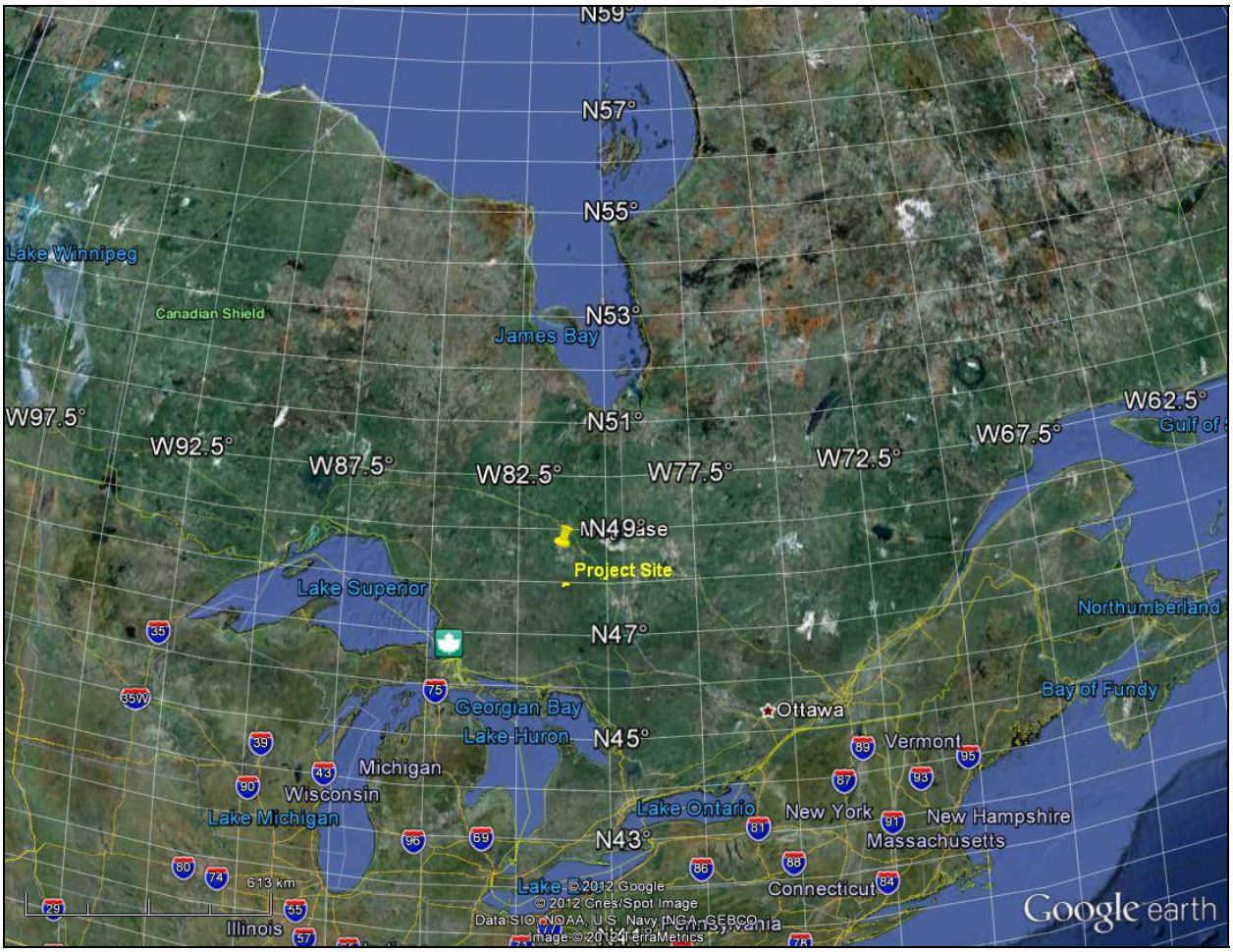

Survey Overview of the Survey Area

APPENDIX B

SURVEY BLOCK COORDINATES
(WGS 84, UTM Zone 17 North)

X	Y
494931	5317150.2
488625.1	5317193.4
488625.1	5318166.4
487530.3	5318200.7
484837.9	5318181
484837.9	5317641.8
483235.9	5317641.8
483235.9	5313985.9
481123.8	5313972.8
481123.8	5310972.9
485200.3	5311002.7
485217.5	5314439.8
486440.8	5314444.6
486440.8	5314845.6
488038.6	5314845.6
488027.4	5315196.3
488625.1	5315166.1
488625.1	5314193.4
494931	5314150.2

APPENDIX C

GEOPHYSICAL MAPS[1]

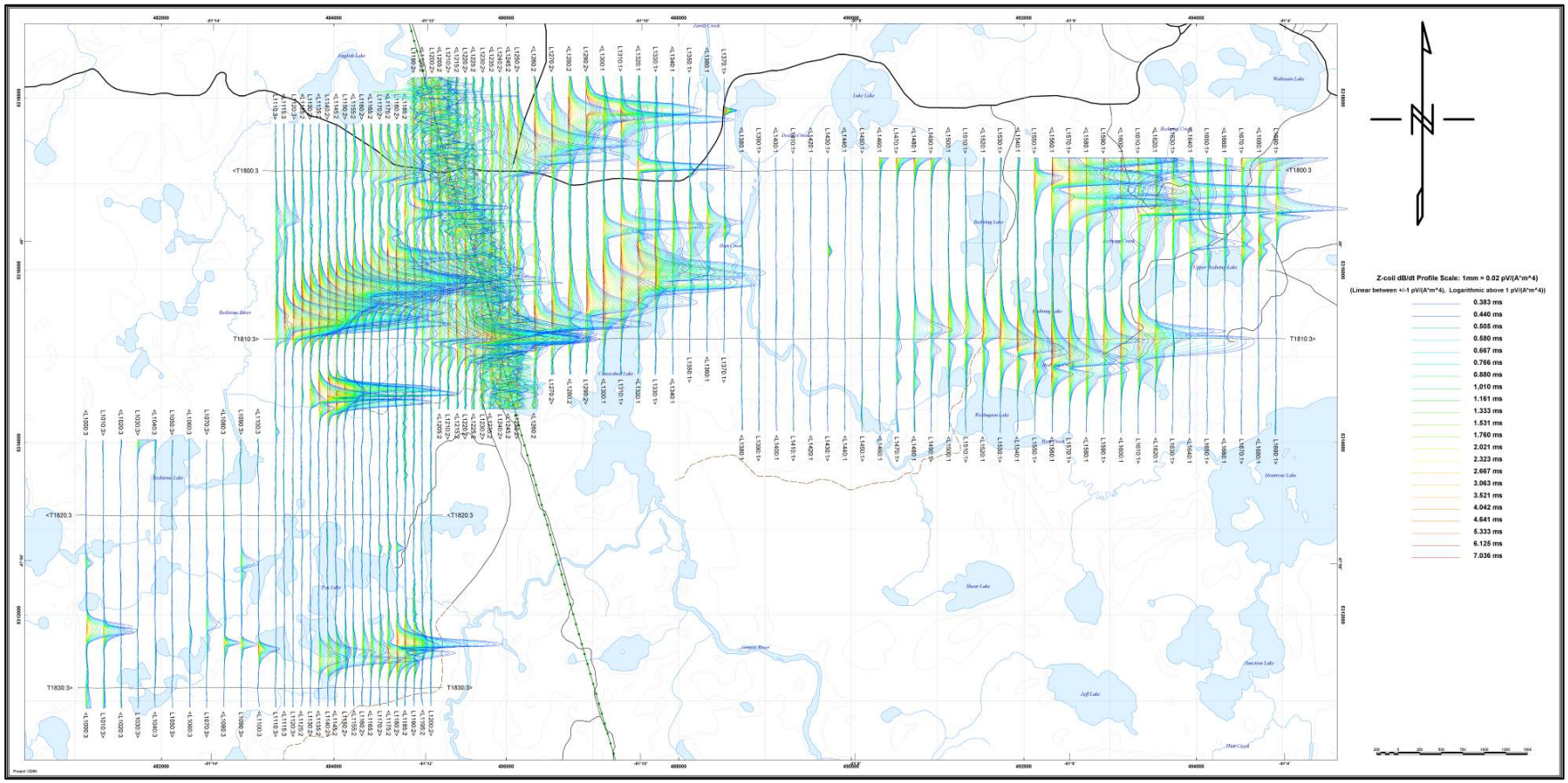

VTEM dB/dt Z Component Profiles, Time Gates 0.220 to 7.036 ms

[1] Full size geophysical maps are also available in PDF format on the final DVD

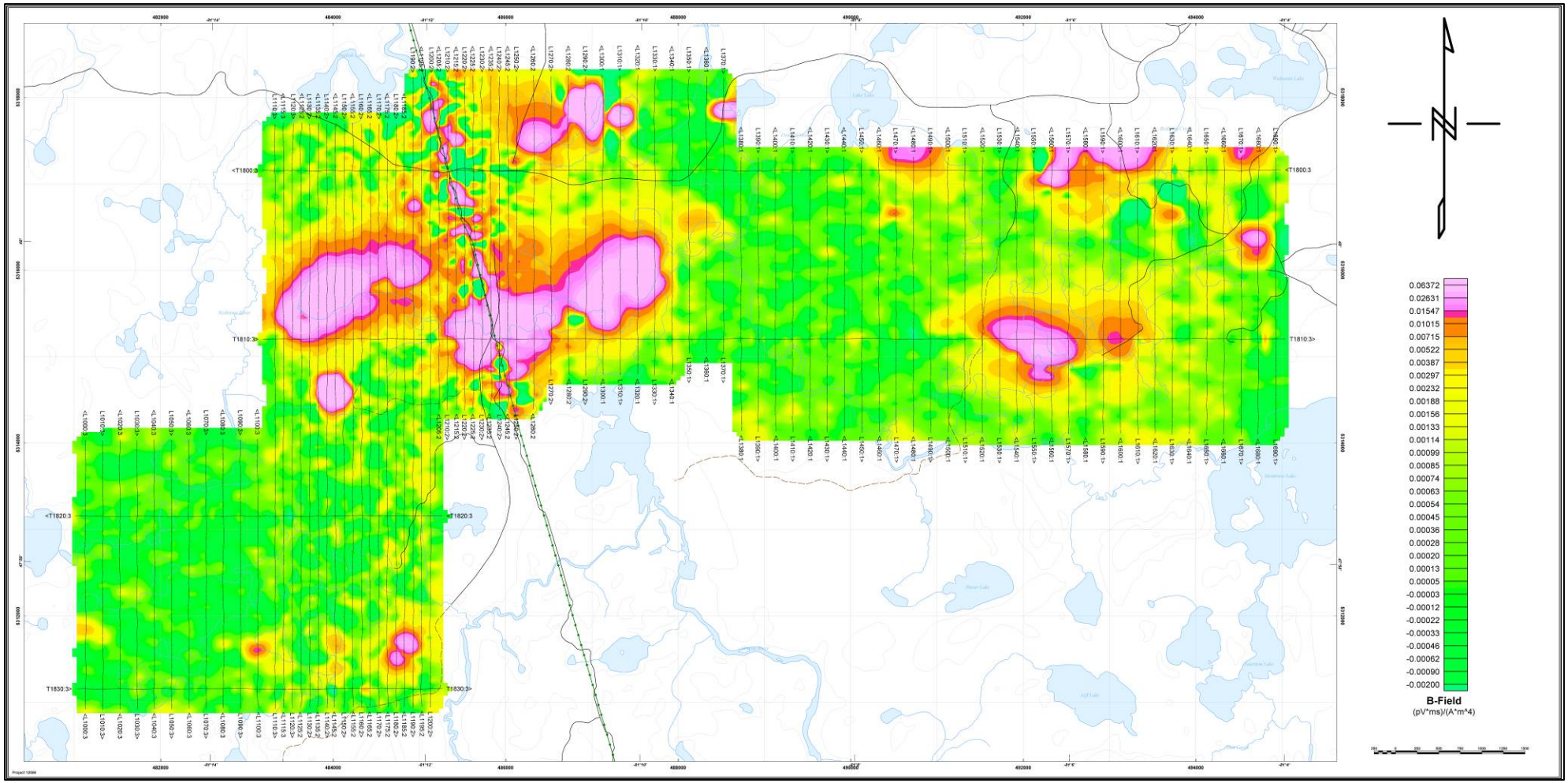

VTEM BField Z Component Channel 44, Time Gate 6.125 ms

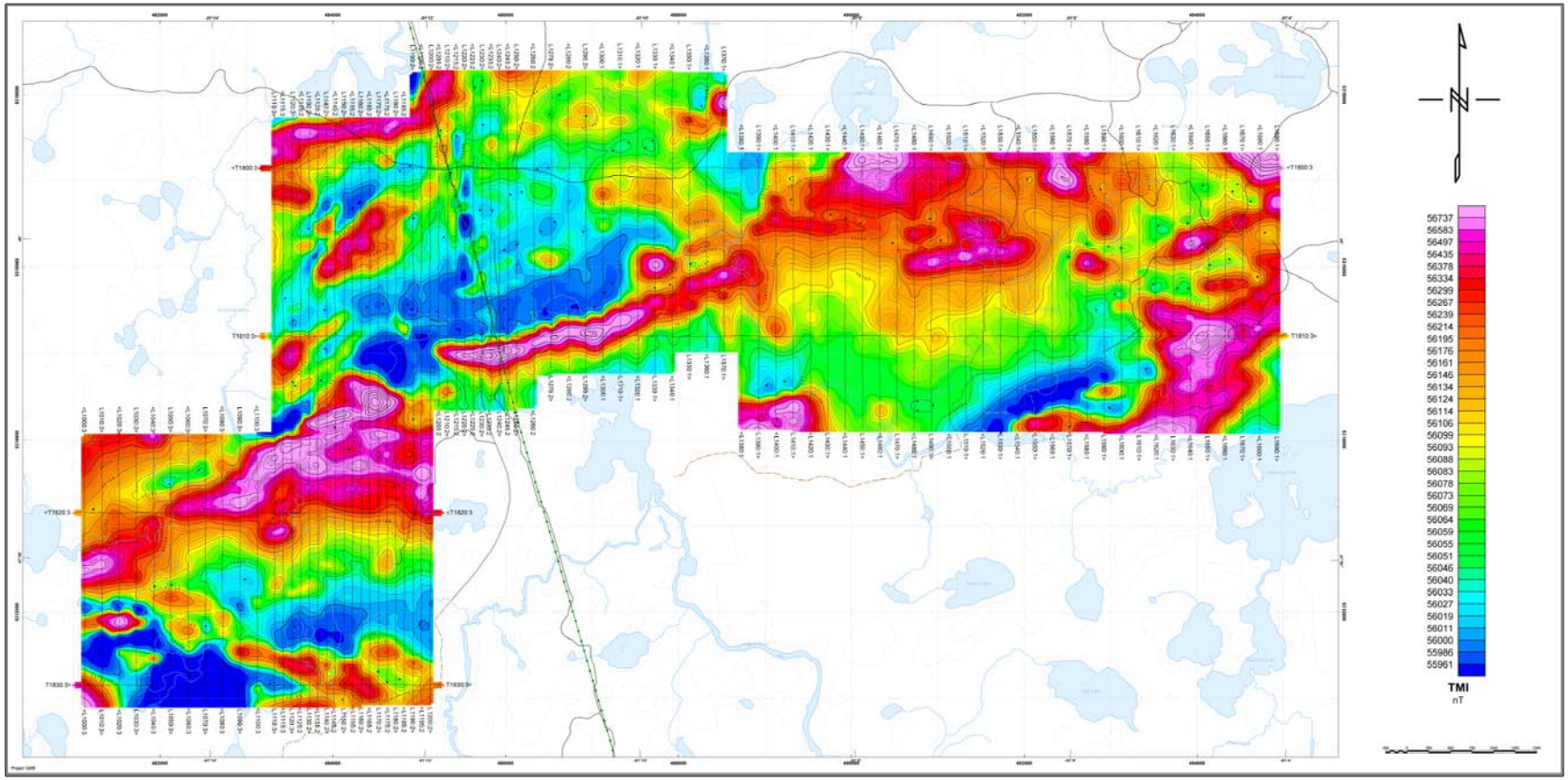

Total Magnetic Intensity (TMI)

APPENDIX D

GENERALIZED MODELING RESULTS OF THE VTEM SYSTEM

Introduction

The VTEM system is based on a concentric or central loop design, whereby, the receiver is positioned at the centre of a transmitter loop that produces a primary field. The wave form is a bi-polar, modified square wave with a turn-on and turn-off at each end.

During turn-on and turn-off, a time varying field is produced (dB/dt) and an electro-motive force (emf) is created as a finite impulse response. A current ring around the transmitter loop moves outward and downward as time progresses. When conductive rocks and mineralization are encountered, a secondary field is created by mutual induction and measured by the receiver at the centre of the transmitter loop.

Efficient modeling of the results can be carried out on regularly shaped geometries, thus yielding close approximations to the parameters of the measured targets. The following is a description of a series of common models made for the purpose of promoting a general understanding of the measured results.

A set of models has been produced for the Geotech VTEM® system dB/dT Z and X components (see models D1 to D15). The Maxwell ™ modeling program (EMIT Technology Pty. Ltd. Midland, WA, AU) used to generate the following responses assumes a resistive half-space. The reader is encouraged to review these models, so as to get a general understanding of the responses as they apply to survey results. While these models do not begin to cover all possibilities, they give a general perspective on the simple and most commonly encountered anomalies.

As the plate dips and departs from the vertical position, the peaks become asymmetrical.

As the dip increases, the aspect ratio (Min/Max) decreases and this aspect ratio can be used as an empirical guide to dip angles from near 90º to about 30º. The method is not sensitive enough where dips are less than about 30º.

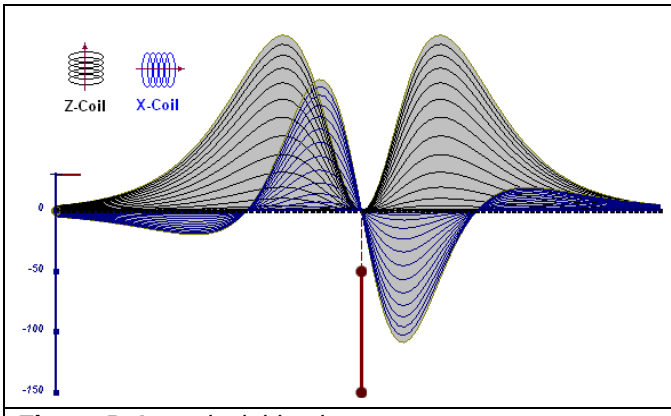

Figure D-1: vertical thin plate

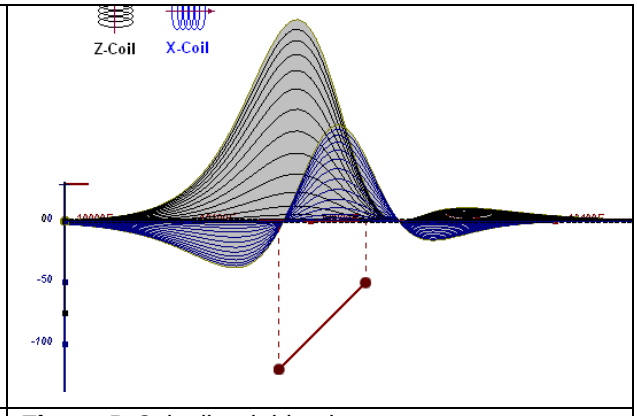

Figure D-2: inclined thin plate

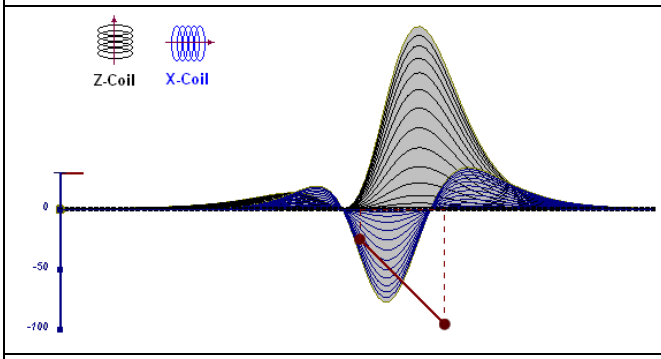

Figure D-3: inclined thin plate

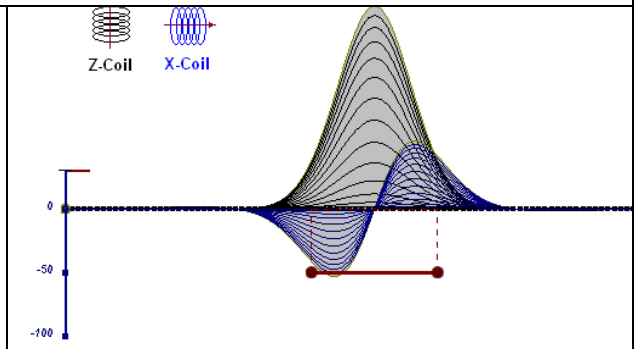

Figure D-4: horizontal thin plate

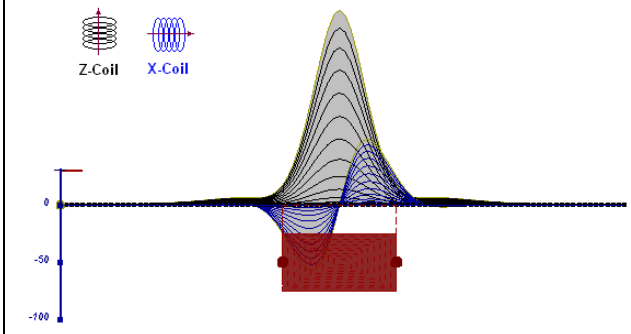

Figure D-5: horizontal thick plate (linear scale of the response)

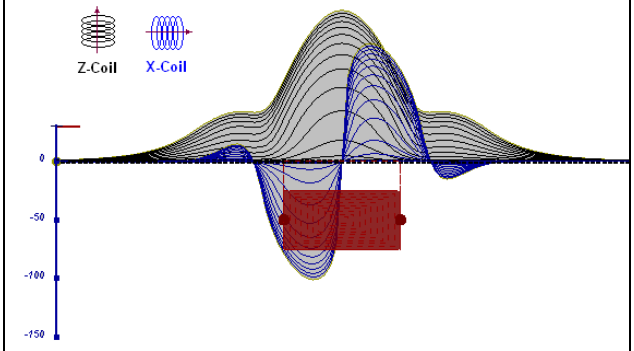

Figure D-6: horizontal thick plate (log scale of the response)

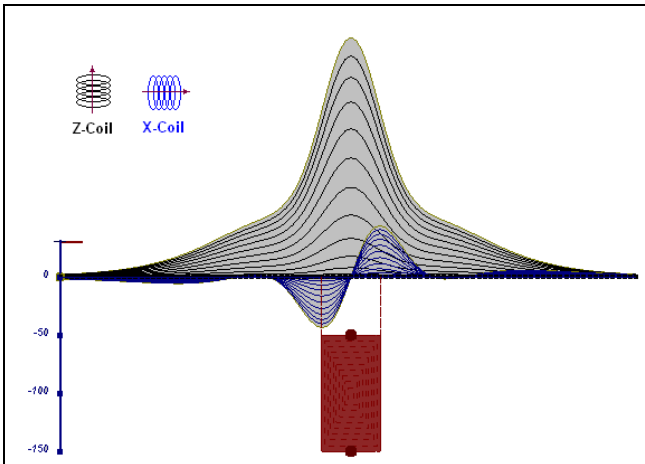

Figure D-7: vertical thick plate (linear scale of the response). 50 m depth

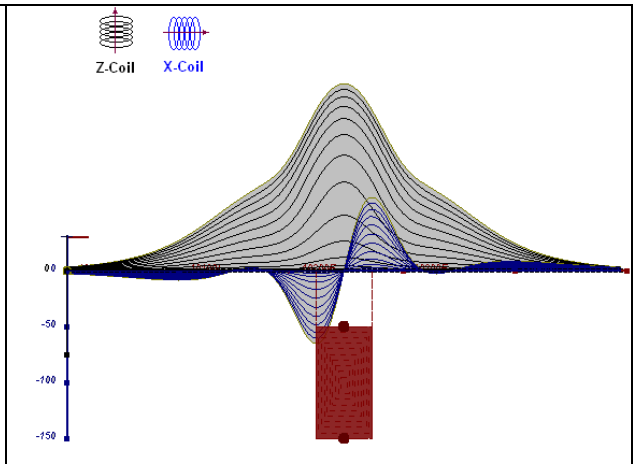

Figure D-8: vertical thick plate (log scale of the response). 50 m depth

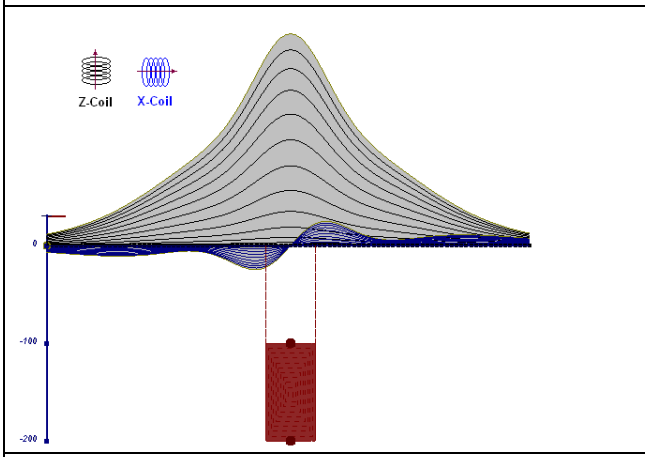

Figure D-9: vertical thick plate (linear scale of the response). 100 m depth

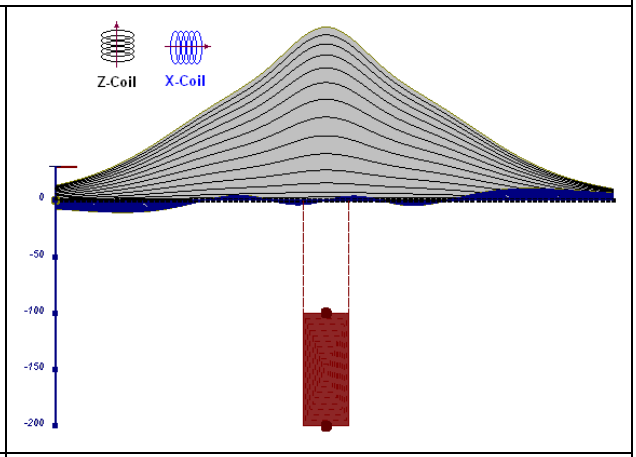

Figure D-10: vertical thick plate (linear scale of the response). Depth/hor.thickness=2.5

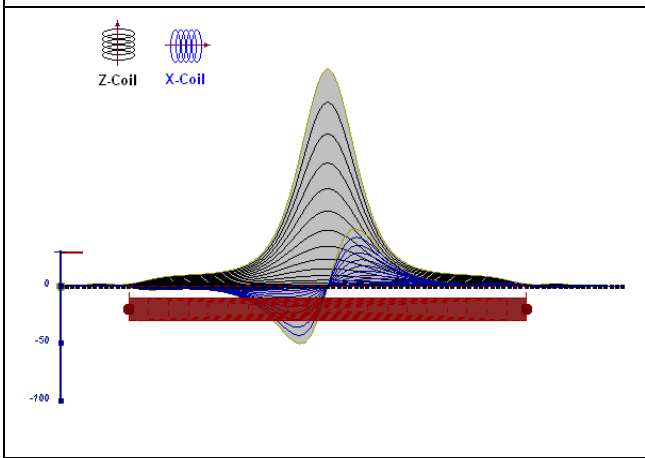

Figure D-10: horizontal thick plate (linear scale of the response)

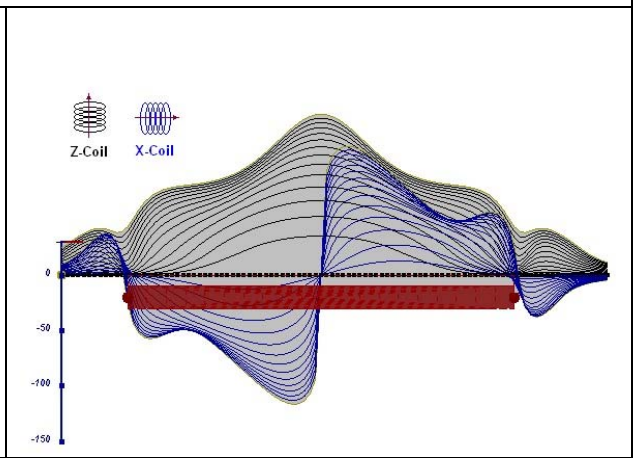

Figure D-11: horizontal thick plate (log scale of the response)

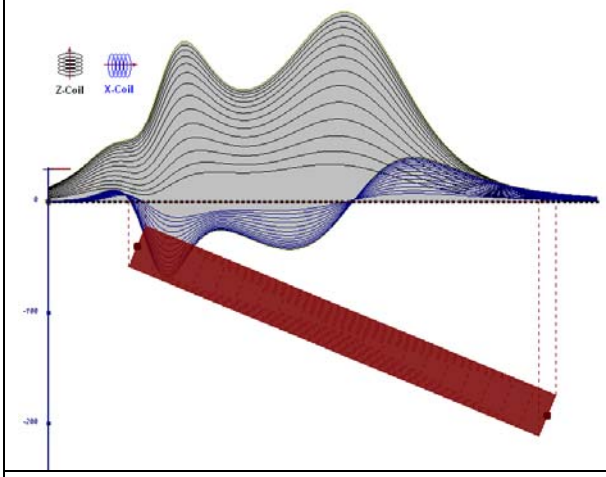

Figure D-12: inclined long thick plate

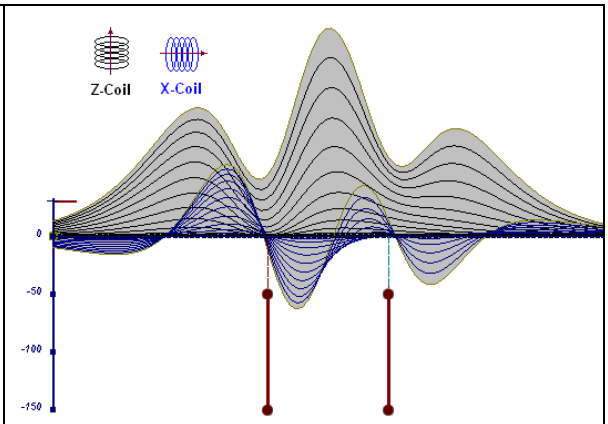

Figure D-13: two vertical thin plates

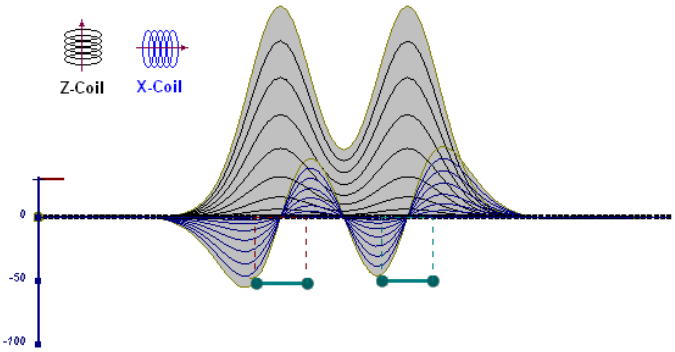

Figure D-14: two horizontal thin plates

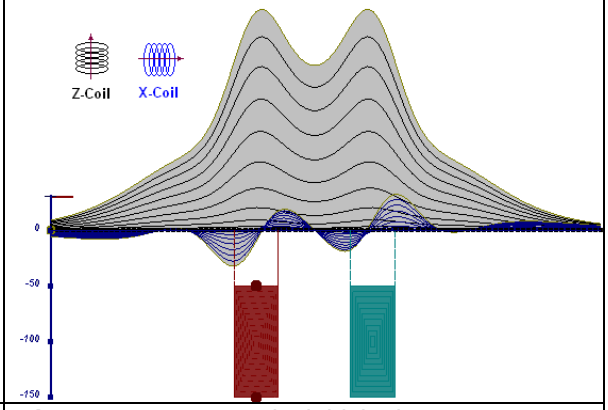

Figure D-15: two vertical thick plates

The same type of target but with different thickness, for example, creates different form of the response:

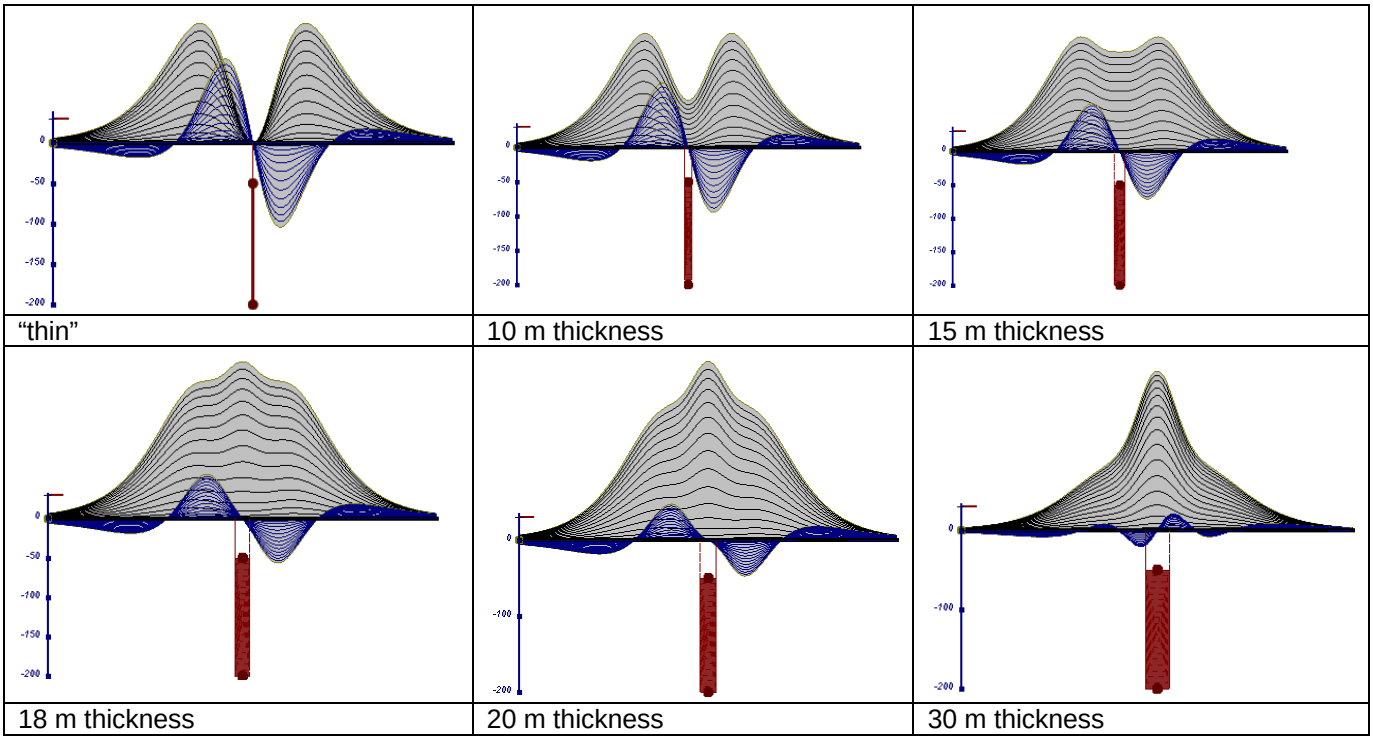

Figure D-16: Conductive vertical plate, depth 50 m, strike length 200 m, depth extends 150 m.

Alexander Prikhodko, PhD, P.Geo
Geotech Ltd.

September 2010

APPENDIX E

EM TIME CONSTANT (TAU) ANALYSIS

Estimation of time constant parameter[1] in transient electromagnetic method is one of the steps toward the extraction of the information about conductances beneath the surface from TEM measurements.

The most reliable method to discriminate or rank conductors from overburden, background or one and other is by calculating the EM field decay time constant (TAU parameter), which directly depends on conductance despite their depth and accordingly amplitude of the response.

Theory

As established in electromagnetic theory, the magnitude of the electro-motive force (emf) induced is proportional to the time rate of change of primary magnetic field at the conductor. This emf causes eddy currents to flow in the conductor with a characteristic transient decay, whose Time Constant (Tau) is a function of the conductance of the survey target or conductivity and geometry (including dimensions) of the target. The decaying currents generate a proportional secondary magnetic field, the time rate of change of which is measured by the receiver coil as induced voltage during the Off time.

The receiver coil output voltage ($\mathbf{e_0}$) is proportional to the time rate of change of the secondary magnetic field and has the form,

$$e_0 \alpha (1 / \tau) e^{-(t/\tau)}$$

Where,
τ = L/R is the characteristic time constant of the target (TAU)
R = resistance
L = inductance

From the expression, conductive targets that have small value of resistance and hence large value of τ yield signals with small initial amplitude that decays relatively slowly with progress of time. Conversely, signals from poorly conducting targets that have large resistance value and smallτ, have high initial amplitude but decay rapidly with time[1] (Fig. E1).

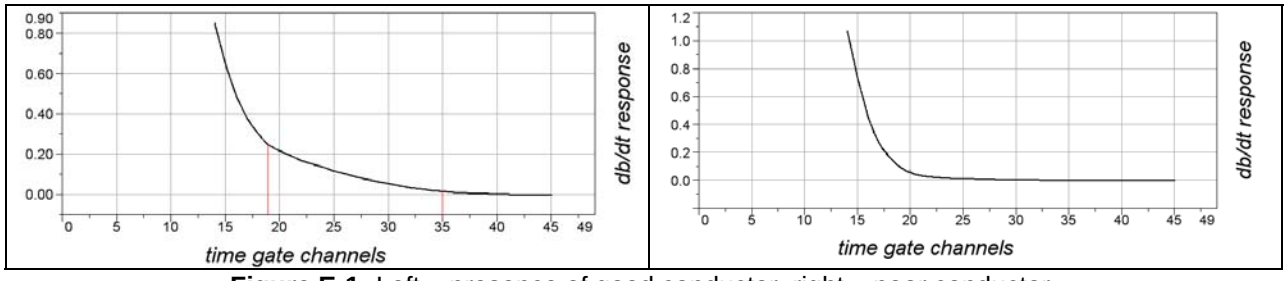

Figure E-1: Left – presence of good conductor, right – poor conductor.

[1] McNeill, JD, 1980, "Applications of Transient Electromagnetic Techniques", Technical Note TN-7 page 5, Geonics Limited, Mississauga, Ontario.

EM Time Constant (Tau) Calculation

The EM Time-Constant (TAU) is a general measure of the speed of decay of the electromagnetic response and indicates the presence of eddy currents in conductive sources as well as reflecting the "conductance quality" of a source. Although TAU can be calculated using either the measured dB/dt decay or the calculated B-field decay, dB/dt is commonly preferred due to better stability (S/N) relating to signal noise. Generally, TAU calculated on base of early time response reflects both near surface overburden and poor conductors whereas, in the late ranges of time, deep and more conductive sources, respectively. For example early time TAU distribution in an area that indicates conductive overburden is shown in Figure 2.

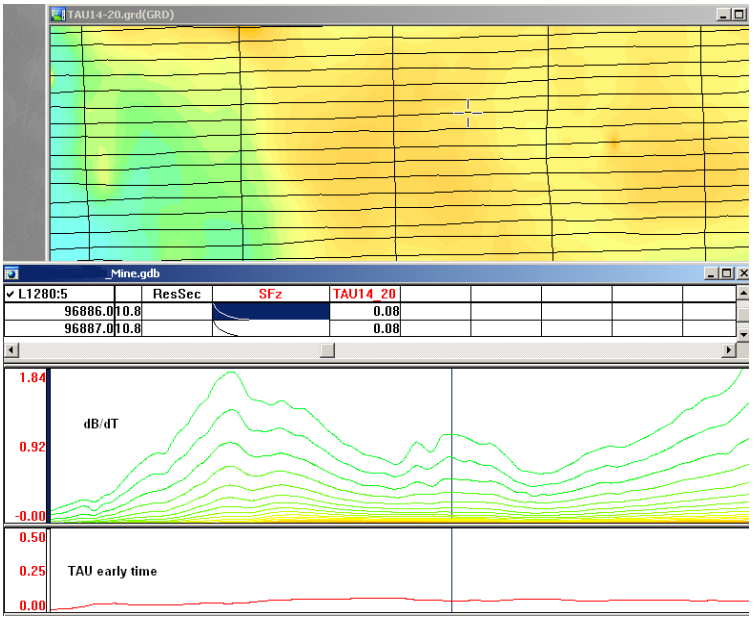

Figure E-2: Map of early time TAU. Area with overburden conductive layer and local sources.

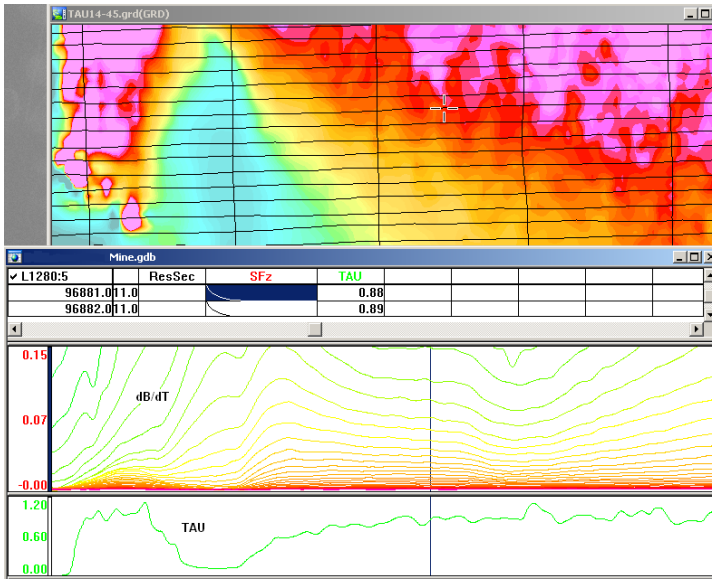

Figure E-3: Map of full time range TAU with EM anomaly due to deep highly conductive target.

There are many advantages of TAU maps:

- TAU depends only on one parameter (conductance) in contrast to response magnitude;
- TAU is integral parameter, which covers time range and all conductive zones and targets are displayed independently of their depth and conductivity on a single map.
- Very good differential resolution in complex conductive places with many sources with different conductivity.
- Signs of the presence of good conductive targets are amplified and emphasized independently of their depth and level of response accordingly.

In the example shown in Figure 4 and 5, three local targets are defined, each of them with a different depth of burial, as indicated on the resistivity depth image (RDI). All are very good conductors but the deeper target (number 2) has a relatively weak dB/dt signal yet also features the strongest total TAU (Figure 4). This example highlights the benefit of TAU analysis in terms of an additional target discrimination tool.

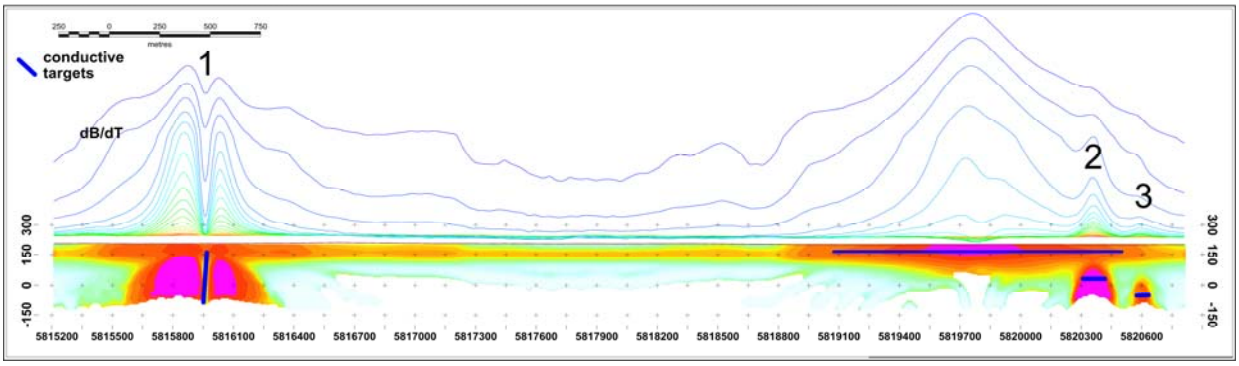

Figure E-4: dB/dt profile and RDI with different depths of targets.

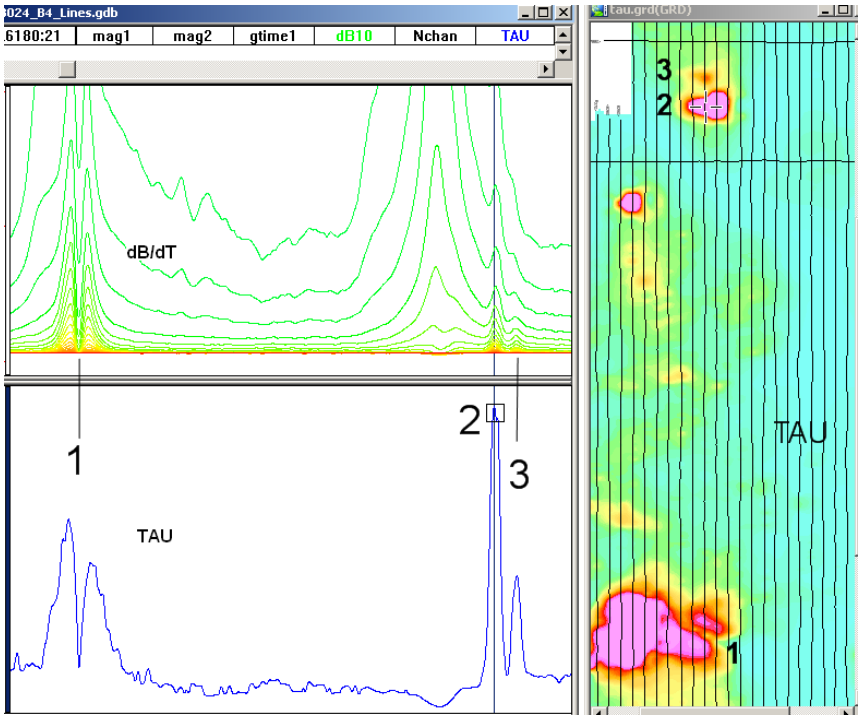

Figure E-5: Map of total TAU and dB/dt profile.

The EM Time Constants for dB/dt and B-field were calculated using the "sliding Tau" in-house program developed at Geotech2. The principle of the calculation is based on using of time window (4 time channels) which is sliding along the curve decay and looking for latest time channels which have a response above the level of noise and decay. The EM decays are obtained from all available decay channels, starting at the latest channel. Time constants are taken from a least square fit of a straight-line (log/linear space) over the last 4 gates above a pre-set signal threshold level (Figure F6). Threshold settings are pointed in the "label" property of TAU database channels. The sliding Tau method determines that, as the amplitudes increase, the time-constant is taken at progressively later times in the EM decay. Conversely, as the amplitudes decrease, Tau is taken at progressively earlier times in the decay. If the maximum signal amplitude falls below the threshold, or becomes negative for any of the 4 time gates, then Tau is not calculated and is assigned a value of "dummy" by default.

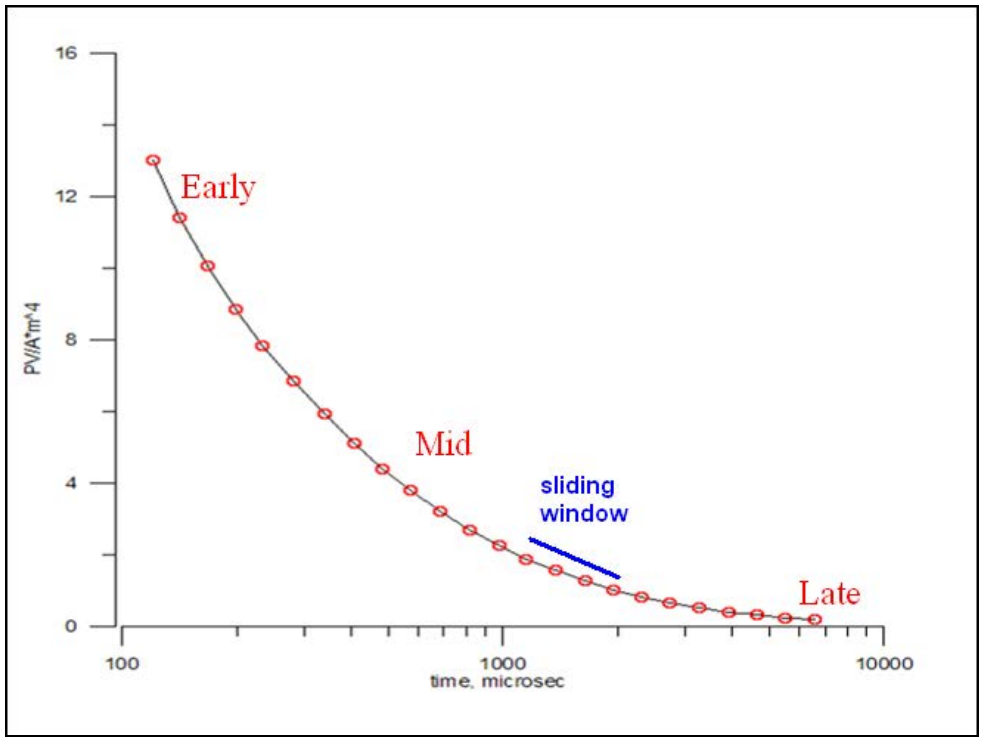

Figure E-6: Typical dB/dt decays of Vtem data

Alexander Prikhodko, PhD, P.Geo
Geotech Ltd.

September 2010

[2] by A.Prikhodko

APPENDIX F

TEM RESISTIVITY DEPTH IMAGING (RDI)

Resistivity depth imaging (RDI) is technique used to rapidly convert EM profile decay data into an equivalent resistivity versus depth cross-section, by deconvolving the measured TEM data.
The used RDI algorithm of Resistivity-Depth transformation is based on scheme of the apparent resistivity transform of Maxwell A.Meju (1998)[1] and TEM response from conductive half-space. The program is developed by Alexander Prikhodko and depth calibrated based on forward plate modeling for VTEM system configuration (Fig. 1-10).

RDIs provide reasonable indications of conductor relative depth and vertical extent, as well as accurate 1D layered-earth apparent conductivity/resistivity structure across VTEM flight lines. Approximate depth of investigation of a TEM system, image of secondary field distribution in half space, effective resistivity, initial geometry and position of conductive targets is the information obtained on base of the RDIs.

Maxwell forward modeling with RDI sections from the synthetic responses (VTEM system)

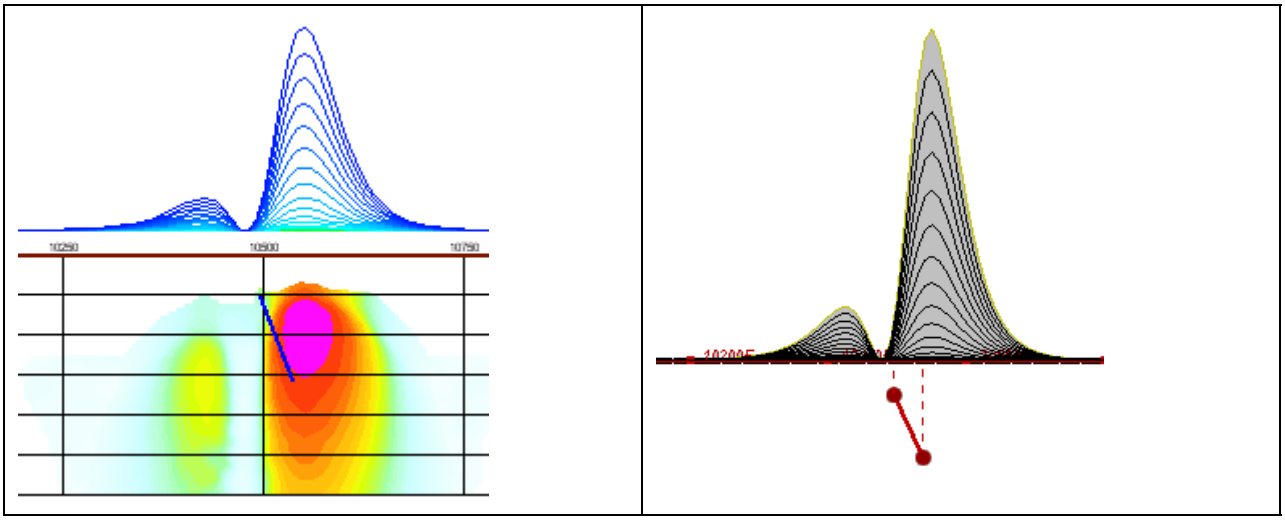

Figure F-1: Maxwell plate model and RDI from the calculated response for conductive “thin” plate (depth 50 m, dip 65 degree, depth extend 100 m).

[1] Maxwell A.Meju, 1998, Short Note: A simple method of transient electromagnetic data analysis, Geophysics, **63**, 405–410.

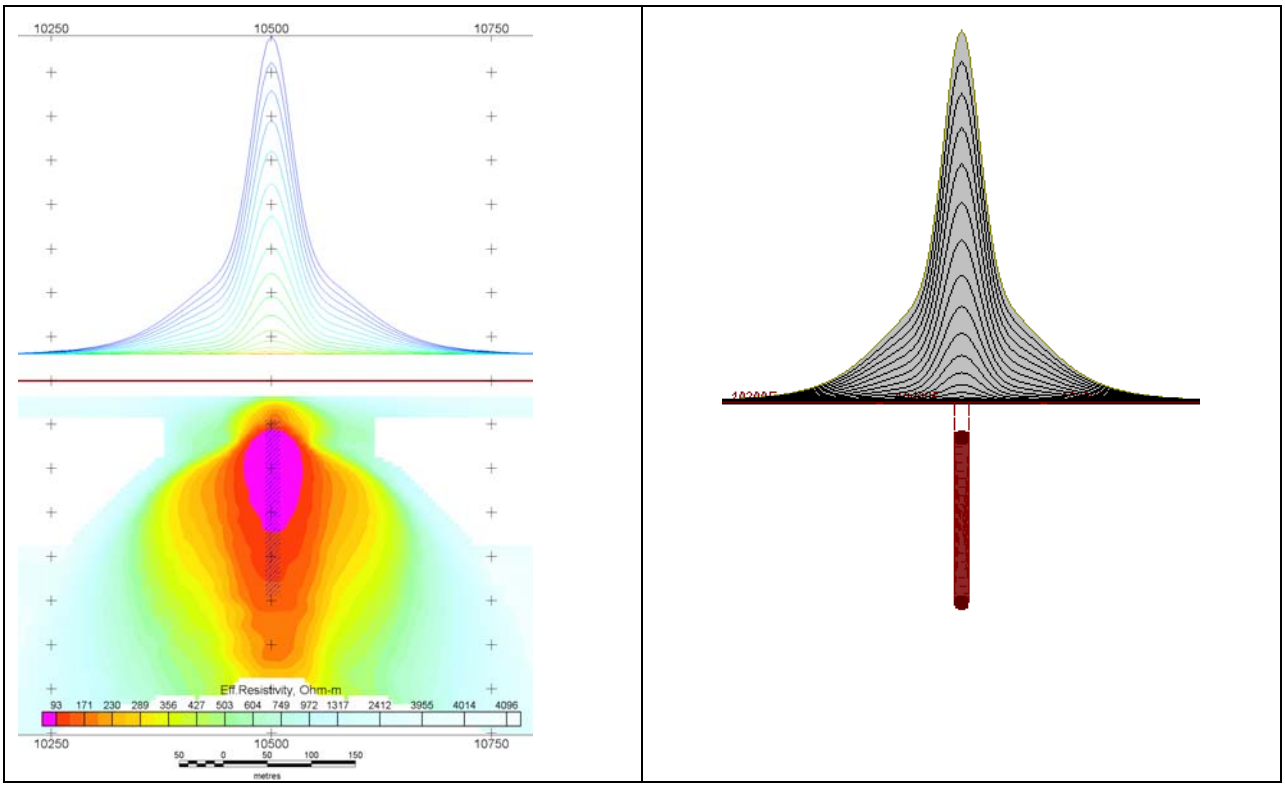

Figure F-2: Maxwell plate model and RDI from the calculated response for "thick" plate 18 m thickness, depth 50 m, depth extend 200 m).

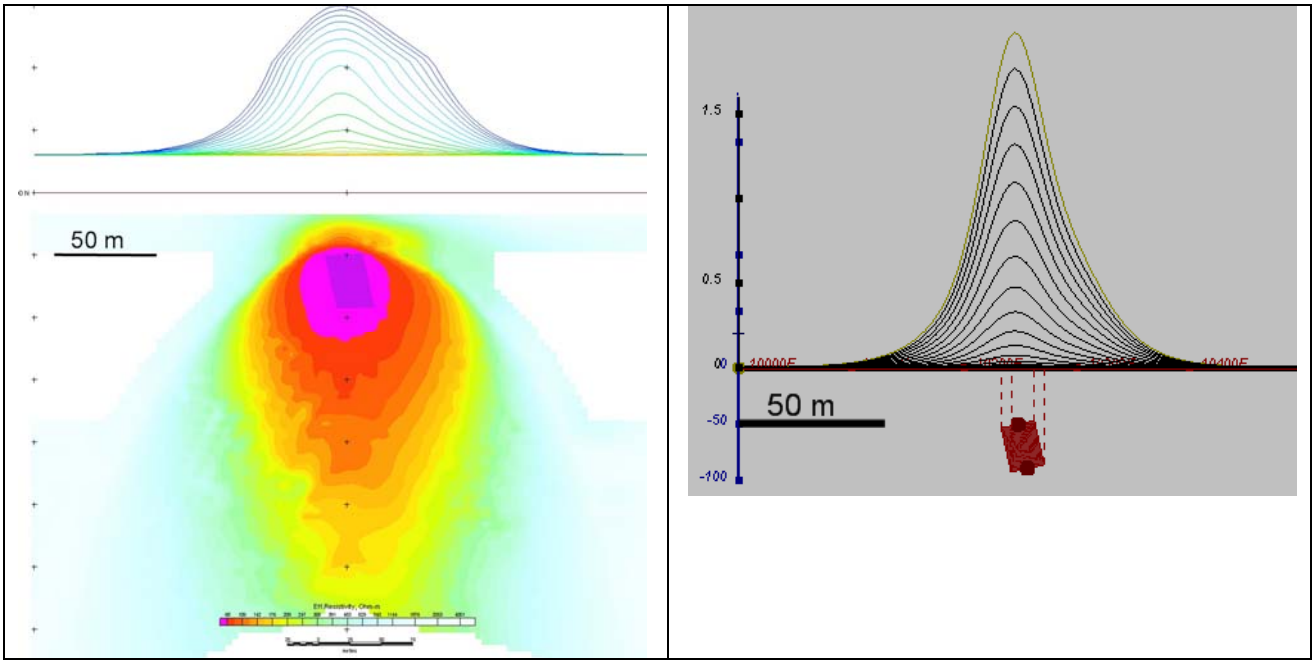

Figure F-3: Maxwell plate model and RDI from the calculated response for bulk ("thick") 100 m length, 40 m depth extend, 30 m thickness

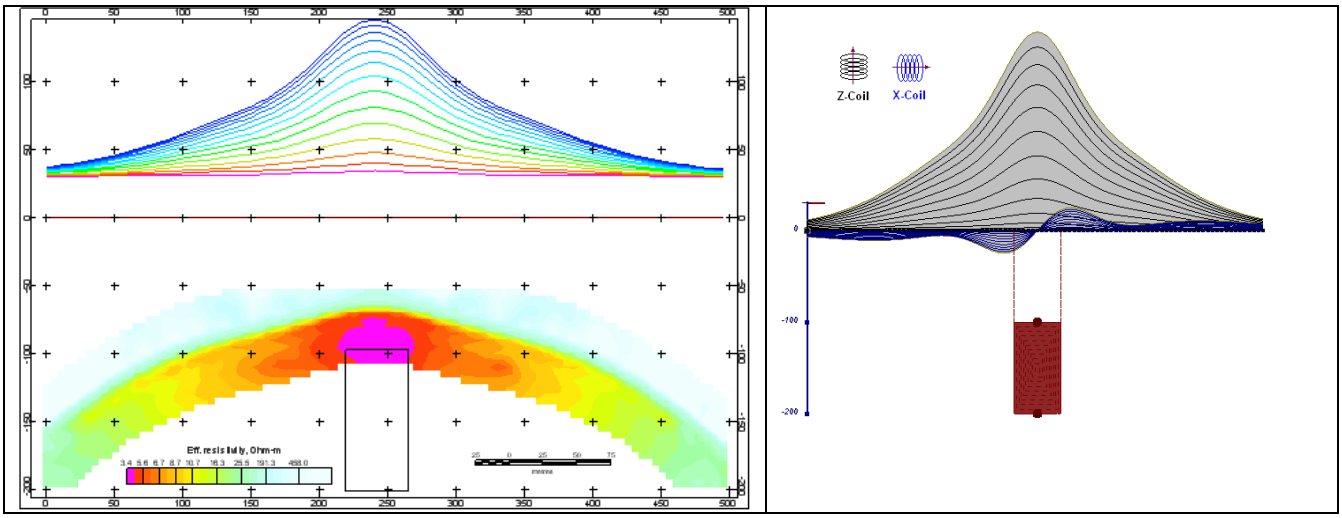

Figure F-4: Maxwell plate model and RDI from the calculated response for "thick" vertical target (depth 100 m, depth extend 100 m). 19-44 chan.

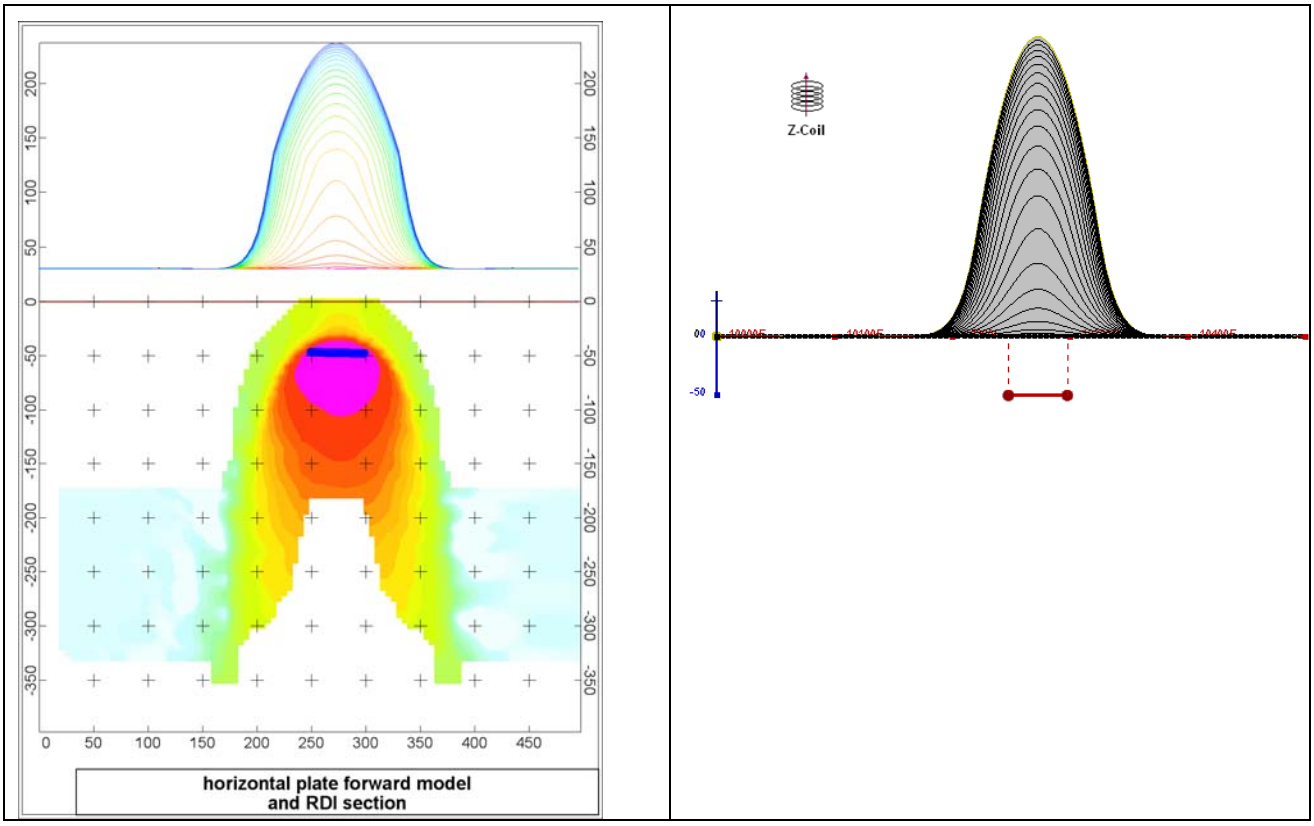

Figure F-5: Maxwell plate model and RDI from the calculated response for horizontal thin plate (depth 50 m, dim 50x100 m). 15-44 chan.

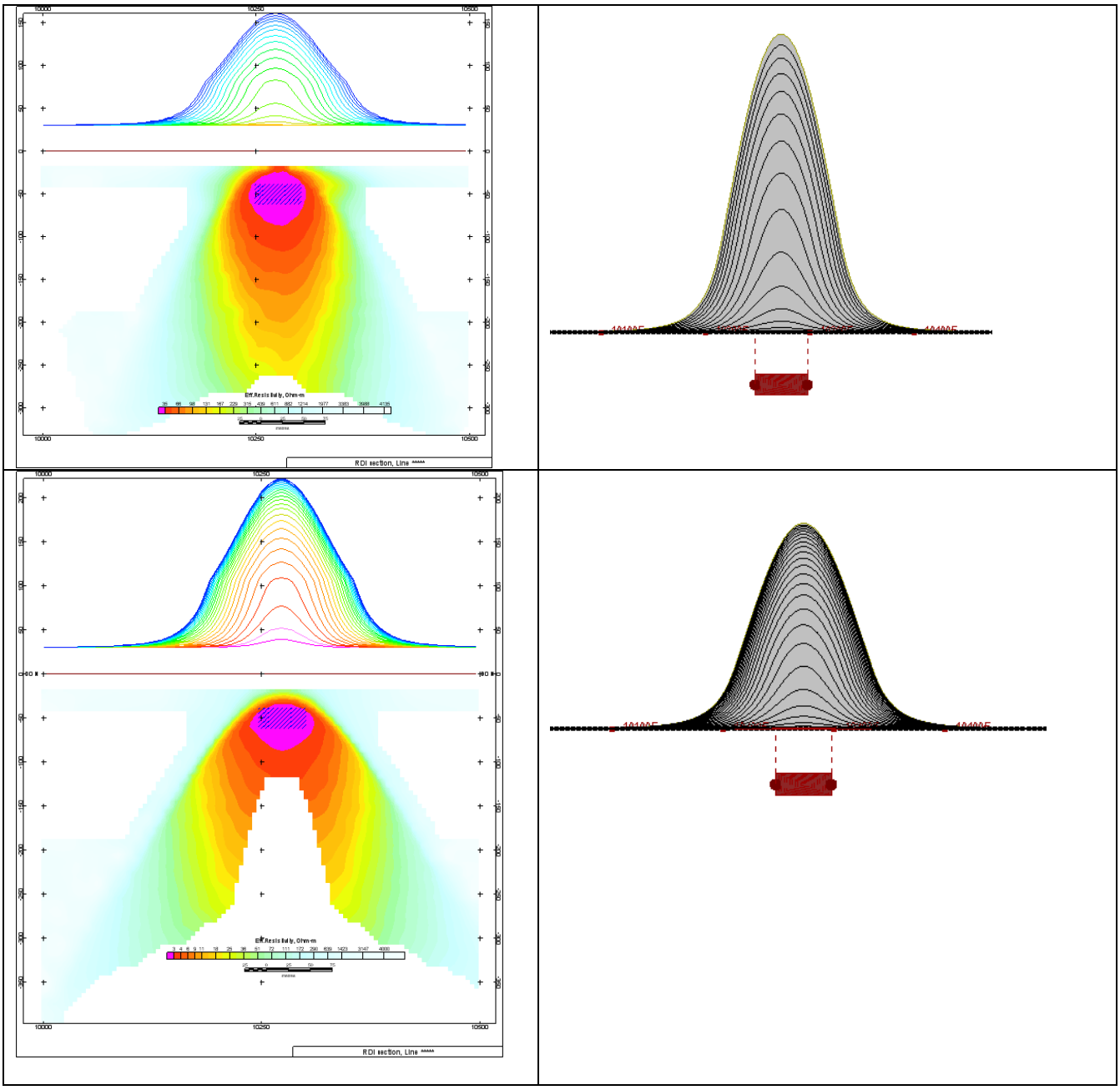

Figure F-6: Maxwell plate model and RDI from the calculated response for horizontal thick (20m) plate – less conductive (on the top), more conductive (below)

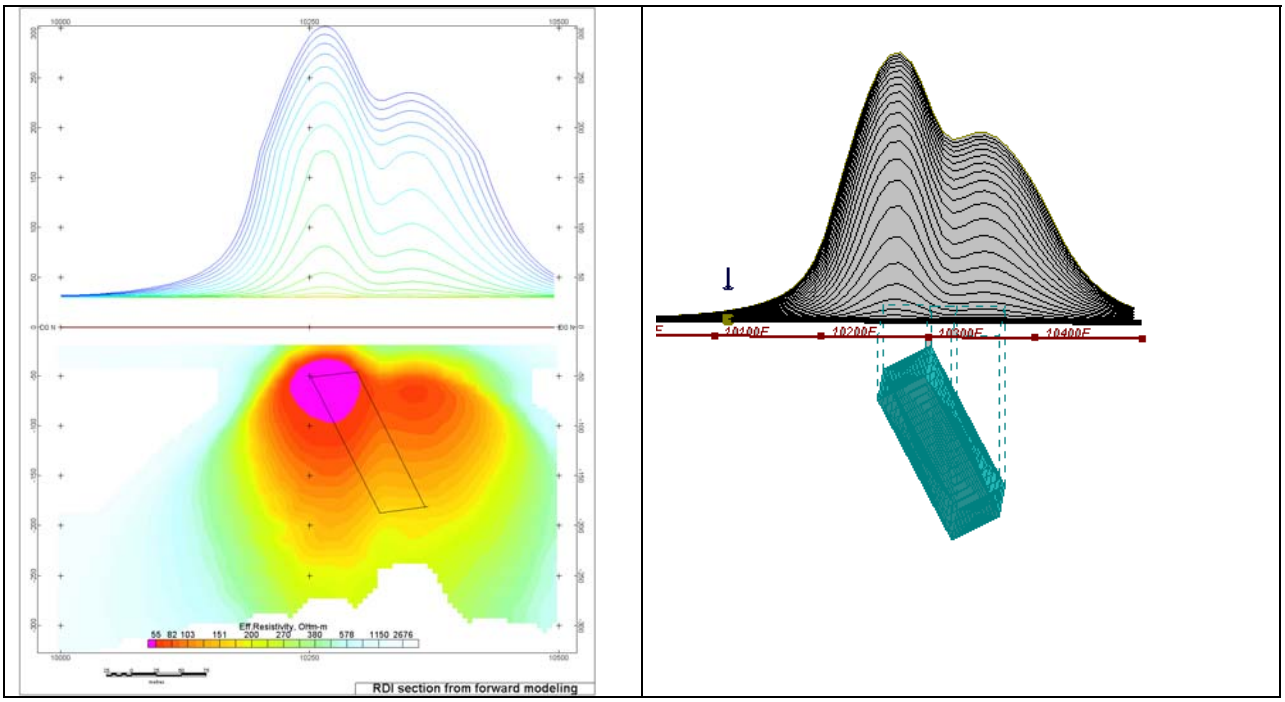

Figure F-7: Maxwell plate model and RDI from the calculated response for inclined thick (50m) plate. Depth extends 150 m, depth to the target 50 m.

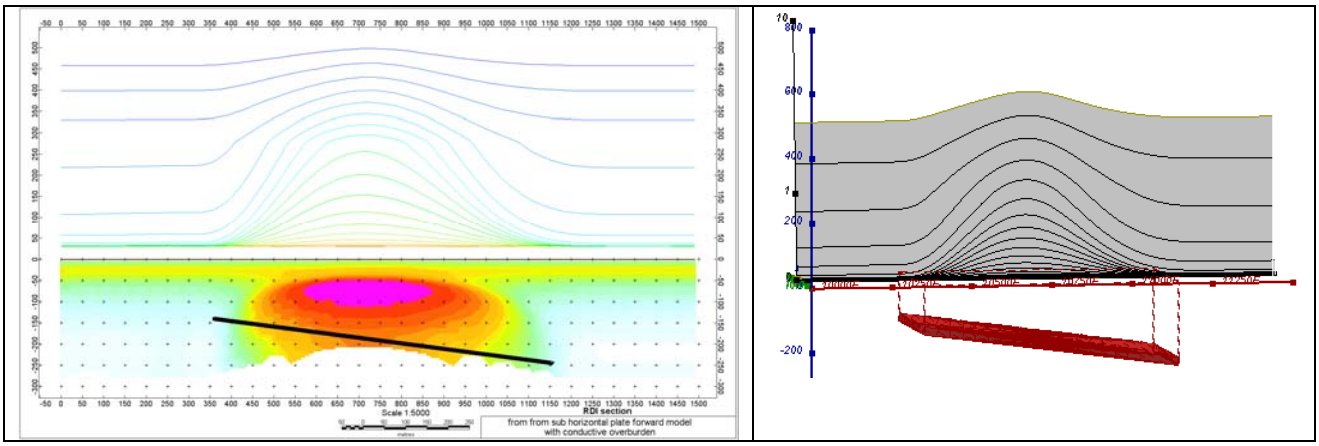

Figure F-8: Maxwell plate model and RDI from the calculated response for the long, wide and deep subhorizontal plate (depth 140 m, dim 25x500x800 m) with conductive overburden.

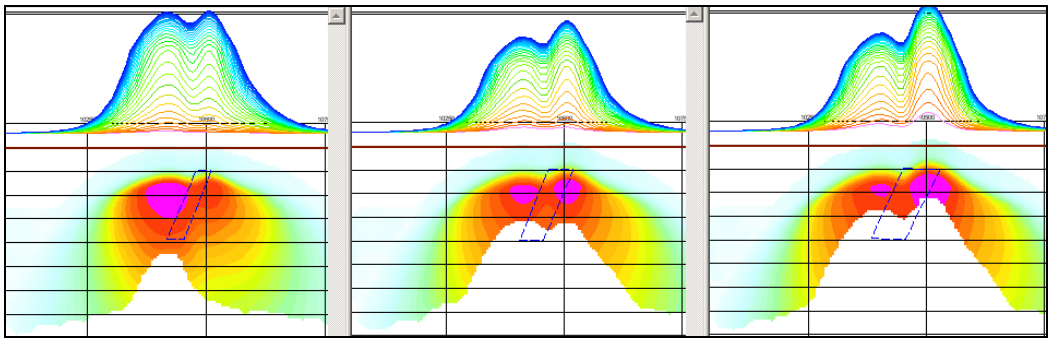

Figure F-9: Maxwell plate models and RDIs from the calculated response for “thick” dipping plates (35, 50, 75 m thickness), depth 50 m, conductivity 2.5 S/m.

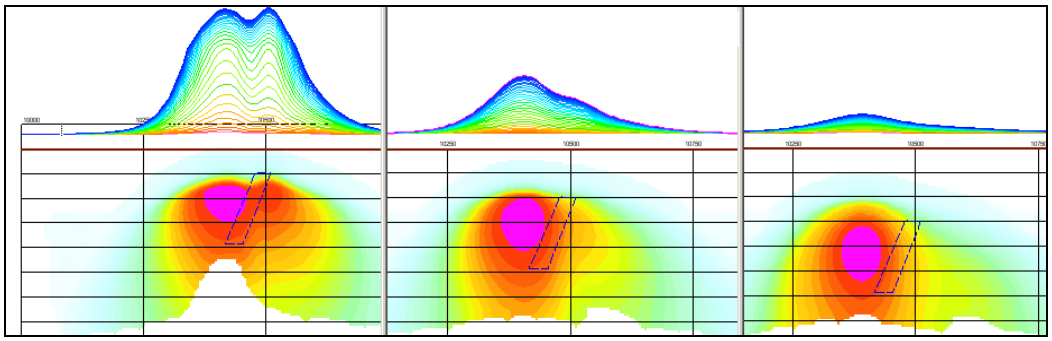

Figure F-10: Maxwell plate models and RDIs from the calculated response for “thick” (35 m thickness) dipping plate on different depth (50, 100, 150 m), conductivity 2.5 S/m.

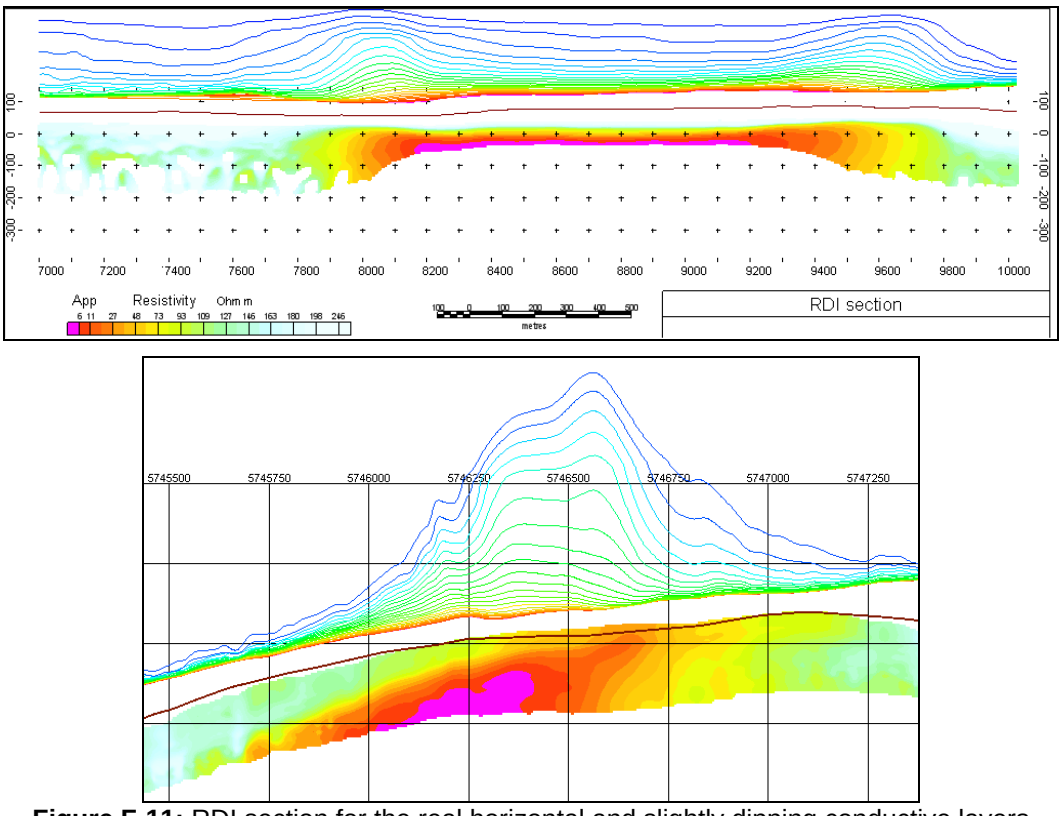

Figure F-11: RDI section for the real horizontal and slightly dipping conductive layers

FORMS OF RDI PRESENTATION

Presentation of series of lines

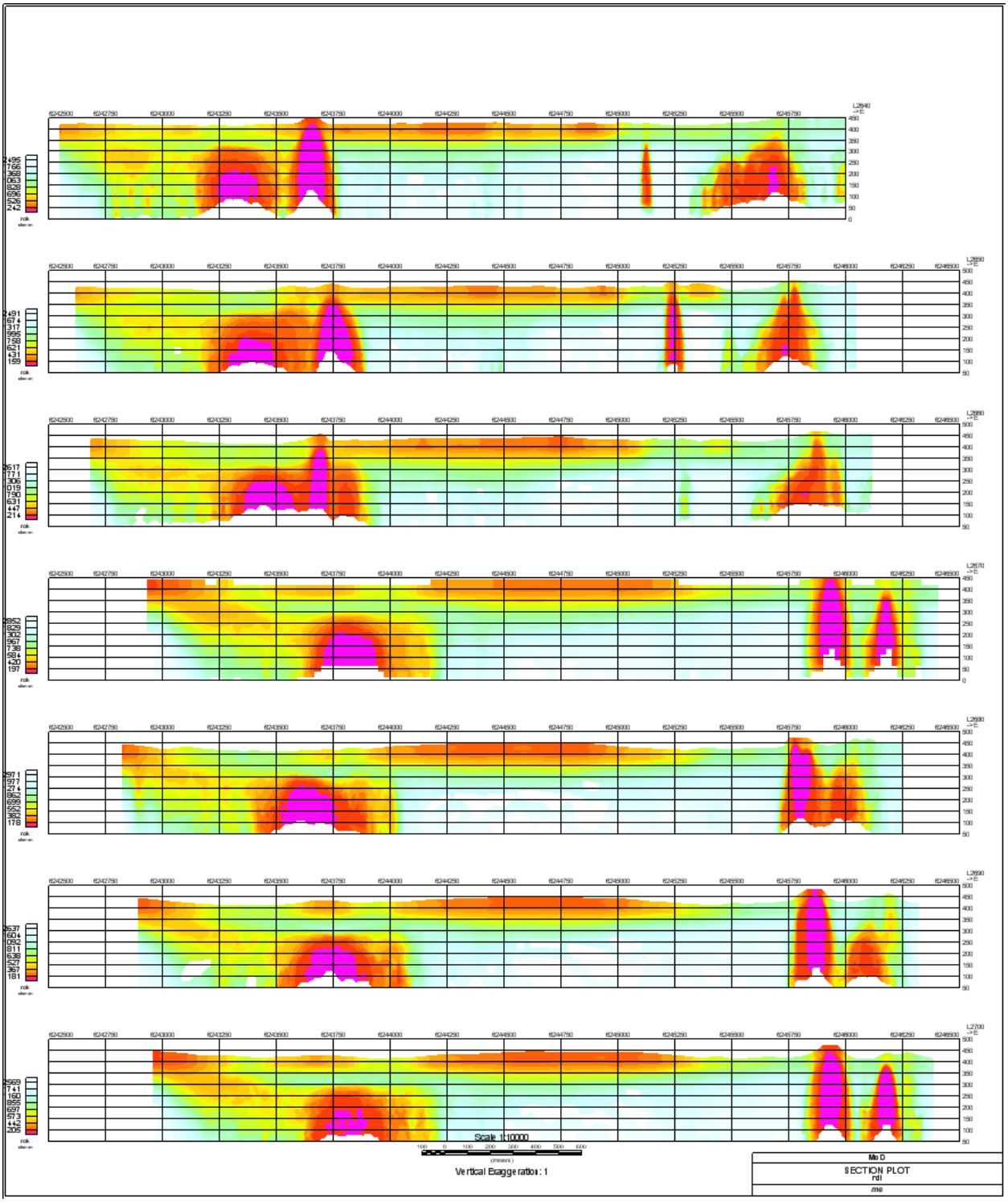

3d presentation of RDIs

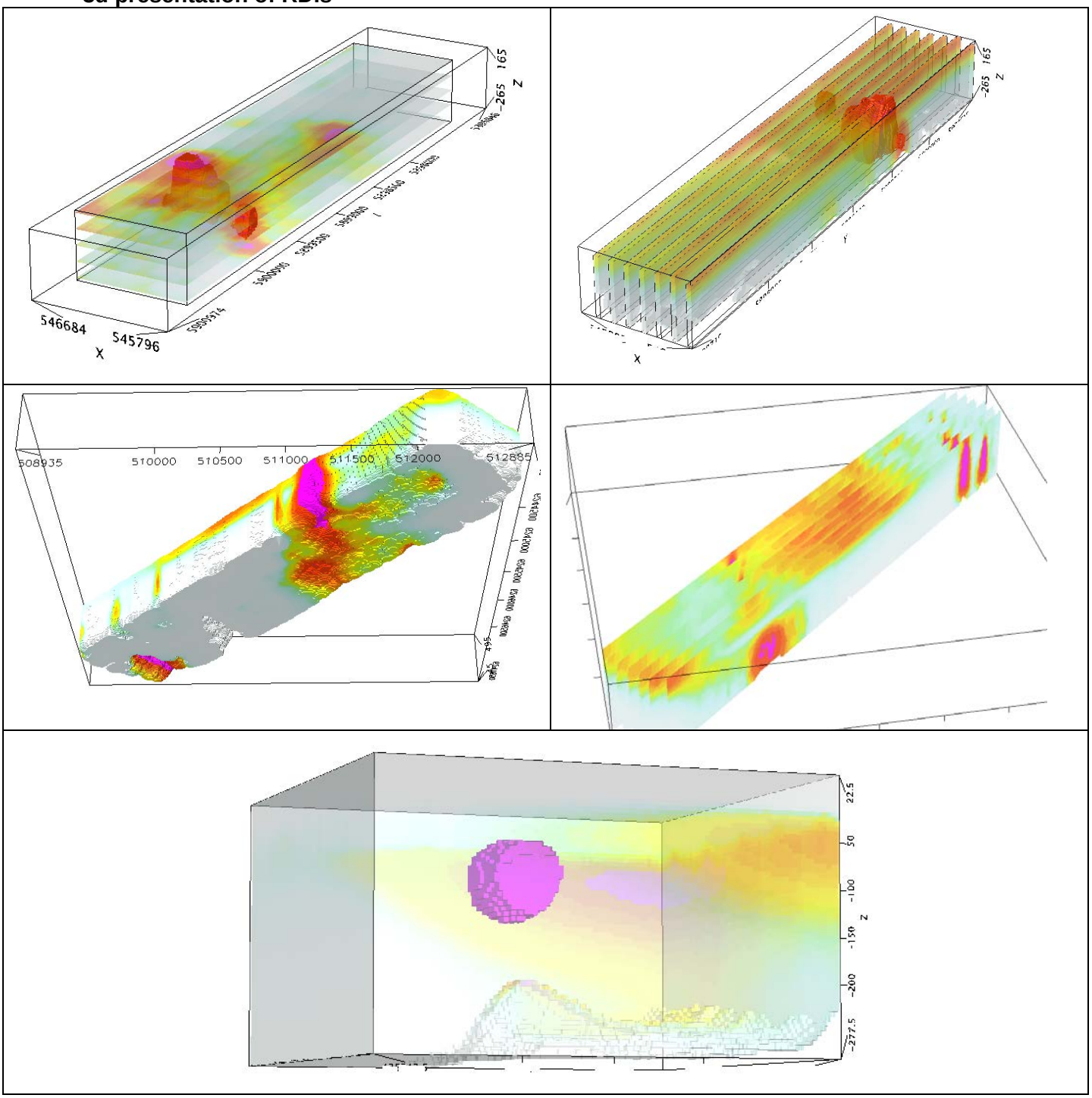

Apparent Resistivity Depth Slices plans:

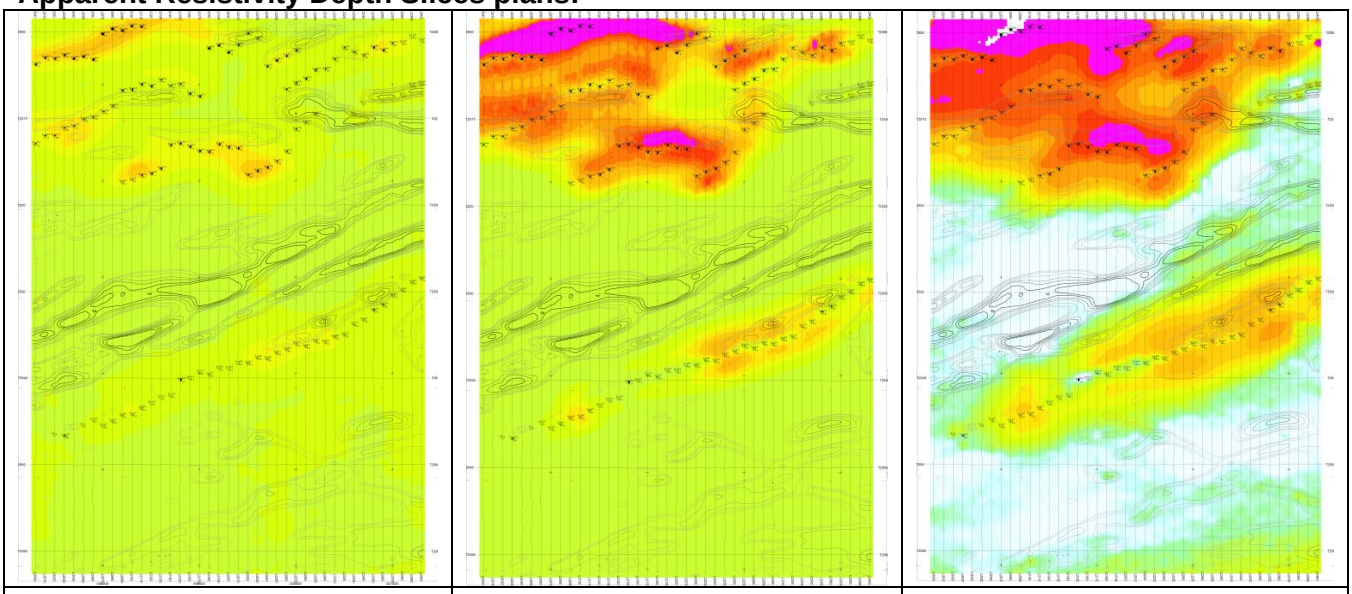

0 m (surface)	-100 m	-200 m

3d views of apparent resistivity depth slices:

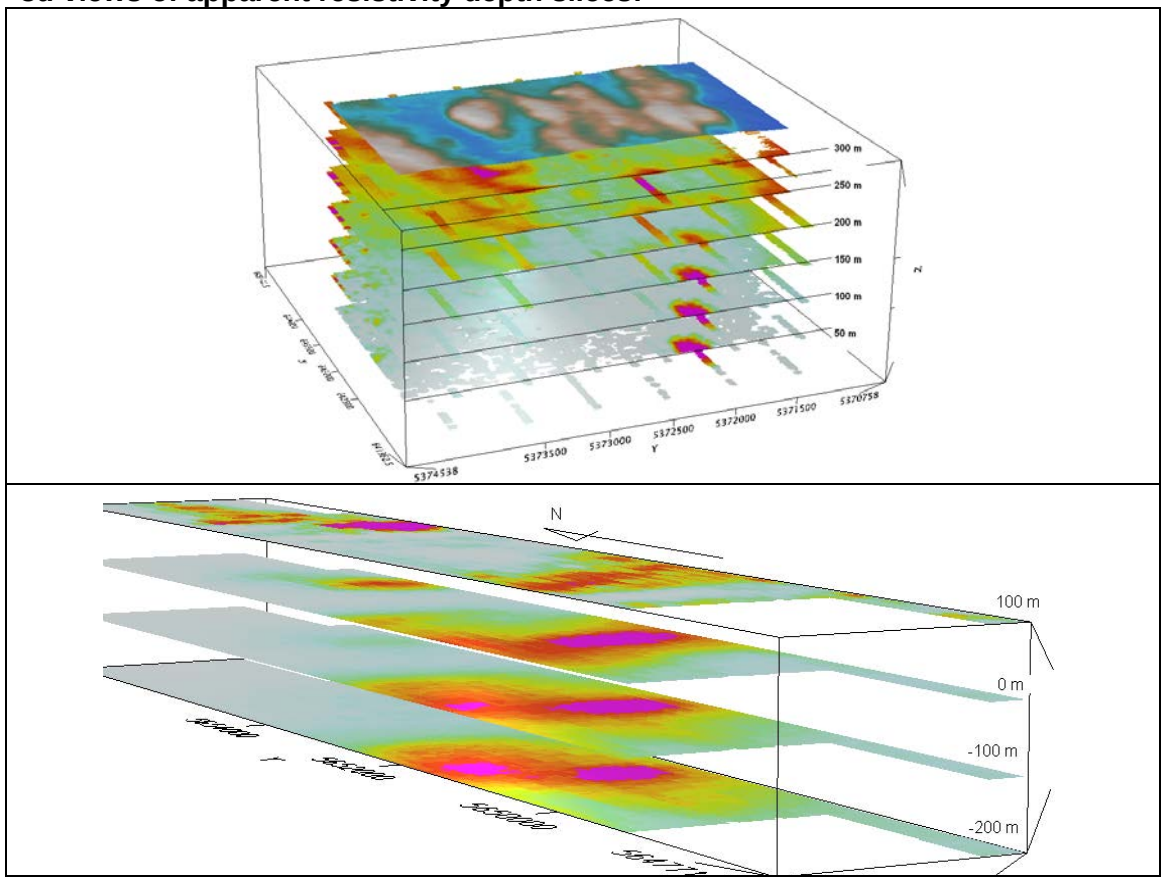

Real base metal targets in comparison with RDIs:

RDI section of the line over Caber deposit ("thin" subvertical plate target and conductive overburden.

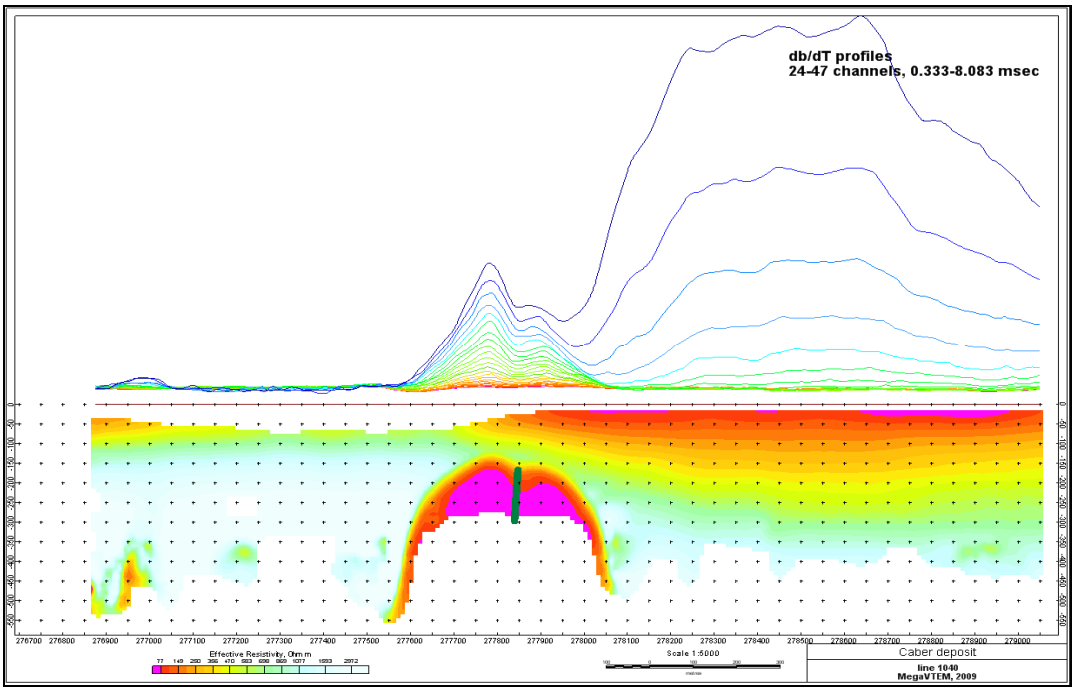

3d RDI voxels with base metals ore bodies (Middle East):

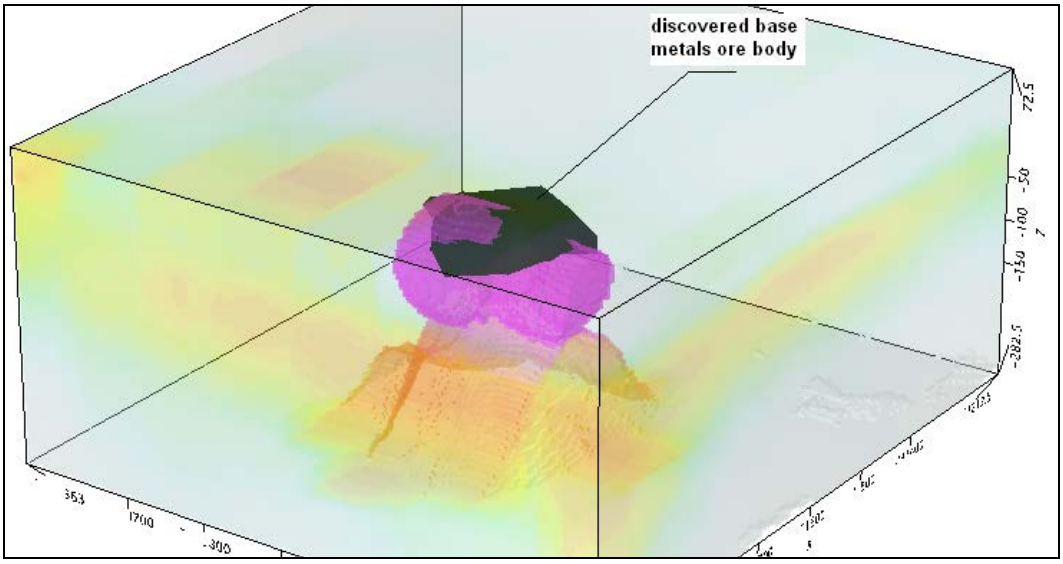

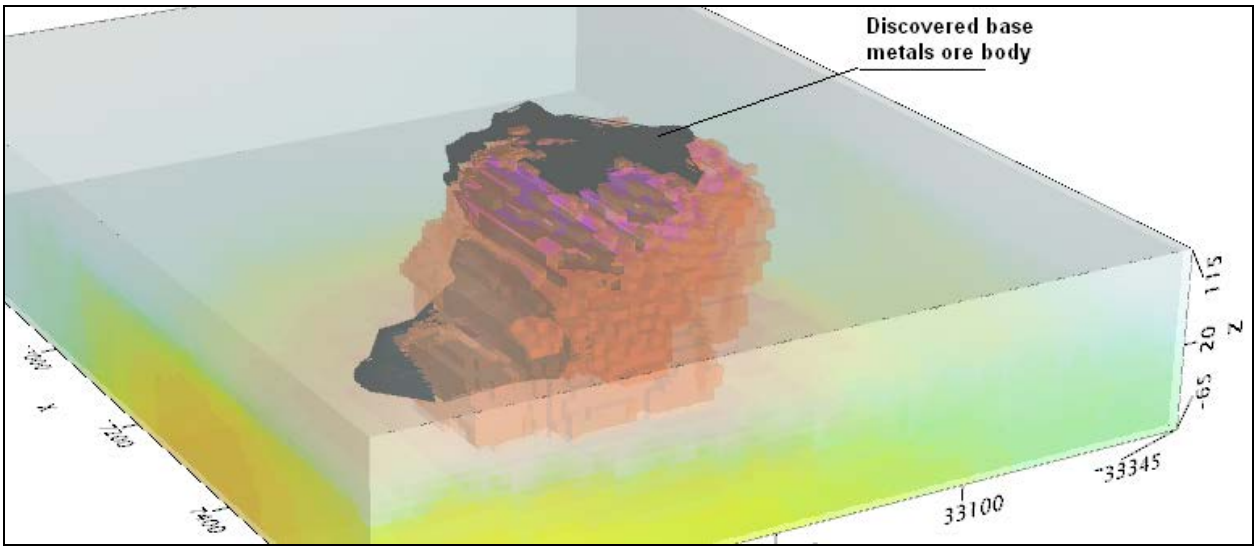

Alexander Prikhodko, PhD, P.Geo
Geotech Ltd.
April 2011